Main Manuscript for

Coordinated molecular and ecological adaptations underlie a highly successful parasitoid

Lan Pang[1,6], Gangqi Fang[2,3,6], Zhiguo Liu[1], Zhi Dong[1], Jiani Chen[1], Ting Feng[1,4], Qichao Zhang[1,4], Yifeng Sheng[1,4], Yueqi Lu[1,4], Ying Wang[1,4], Yixiang Zhang[2,3], Guiyun Li[2], Xuexin Chen[1,4,5], Shuai Zhan[2,3*], Jianhua Huang[1,4*]

[1]Institute of Insect Sciences, Ministry of Agriculture Key Lab of Molecular Biology of Crop Pathogens and Insect Pests, College of Agriculture and Biotechnology, Zhejiang University, Hangzhou, China

[2]CAS Key Laboratory of Insect Developmental and Evolutionary Biology, CAS Center for Excellence in Molecular Plant Sciences, Chinese Academy of Sciences, Shanghai, China

[3]CAS Center for Excellence in Biotic Interactions, University of Chinese Academy of Sciences, Beijing, China

[4]Key Laboratory of Biology of Crop Pathogens and Insects of Zhejiang Province, Zhejiang University, Hangzhou, China

[5]State Key Lab of Rice Biology, Zhejiang University, Hangzhou, China

[6]These authors contributed equally

*Corresponding authors: Shuai Zhan, Jianhua Huang

Email: szhan@sibs.ac.cn (S.Z.); jhhuang@zju.edu.cn (J.H.)

Abstract

The success of an organism depends on the molecular and ecological adaptations that promote its beneficial fitness. Parasitoids are valuable biocontrol agents for successfully managing agricultural pests, and they have evolved diversified strategies to adapt to both the physiological condition of hosts and the competition of other parasitoids. Here, we deconstructed the parasitic strategies in a highly successful parasitoid, *Trichopria drosophilae*, which parasitizes a broad range of *Drosophila* hosts, including the globally invasive species *D. suzukii*. We found that *T. drosophilae* had developed specialized venom proteins that arrest host development to obtain more nutrients via secreting tissue inhibitors of metalloproteinases (TIMPs), as well as a unique type of cell—teratocytes—that digest host tissues for feeding by releasing trypsin proteins. In addition to the molecular adaptations that optimize nutritional uptake, this pupal parasitoid has evolved ecologically adaptive strategies including the conditional tolerance of intraspecific competition to enhance parasitic success in older hosts and the obligate avoidance of interspecific competition with larval parasitoids. Our study not only demystifies how parasitoids weaponize themselves to colonize formidable hosts but also provided empirical evidence of the intricate coordination between the molecular and ecological adaptations that drive evolutionary success.

Introduction

It is estimated that approximately 10% of insect species are parasitoids, with females typically depositing their eggs either in (endoparasitoids) or on (ectoparasitoids) the bodies of their hosts, leading to the consumption of the host by the parasitoid's developing offspring (Eggleton et al., 1992; Vinson and Iwantsch, 1980; Charnov, 1994; Harvey and Strand, 2002; Pennacchio and Strand, 2006; van de Kamp et al., 2018). The antagonistic coevolution between parasitoids and hosts has spurred a vast array of adaptive and counter-adaptive strategies, in which the hosts have developed better immune responses and/or evasion behaviours to prevent parasitism; however, parasitoids have evolved diversified parasitic strategies to enable successful parasitism (Müller and Schmid-Hempel, 1993; Kacsoh et al., 2013; Huang et al., 2021; Chen et al., 2021; Pang et al., 2022; Wertheim, 2022). This evolutionary arms race fosters a dynamic ecosystem characterized by either the emergence of strong resistance mechanisms in certain host species or the evolution of powerful parasitic strategies in certain parasitoids (Beckage and Gelman, 2004; Colinet et al., 2007; Wang et al., 2018b; Gasmi et al., 2021).

One example notable for strong resistance to parasitization is the spotted-wing fruit fly *Drosophila suzukii* (Diptera: Drosophilidae). This invasive species originated in Asia and has spread rapidly throughout the world over the last decade, with records in Europe (since 2008), North America (since 2008), South America (since 2013), and Africa (since 2017) (Deprá et al., 2014; Dos Santos et al., 2017; Boughdad et al., 2021). *D. suzukii* attacks a broad spectrum of soft-skinned fruits and causes serious economic damage to fruit and wine production (Rota-Stabelli et al., 2013; Asplen et al., 2015; Knapp et al., 2021). Despite the broad interest in seeking natural

enemies, the most well-recognized drosophilid parasitoids cannot parasitize *D. suzukii* (Chabert et al., 2012; Poyet et al., 2013; Lee et al., 2019).

We conducted field investigations to identify natural parasitoids of *D. suzukii* from 2016 to 2020. We placed traps containing the favourite fruits of *D. suzukii* (e.g. banana pieces, cherries, and grapes) on *Myrica rubra* trees at several locations in East China (e.g. Hangzhou, Ningbo, and Taizhou), where *D. suzukii* is heavily distributed (Wang et al., 2020; Yu et al., 2021). Among the reclaimed parasitic wasps, we primarily characterized two species: *Trichopria drosophilae* (Td) (Hymenoptera: Diapriidae), which parasitizes *D. suzukii* pupae, and *Asobara japonica* (Aj) (Braconidae), which parasitizes larvae. Remarkably, we observed a constant proportion of Td in repeated traps, which attracted the most interest. The parasitic success of Td on *D. suzukii* has been documented in the USA and Europe independently (Knoll et al., 2017; Wang et al., 2018a; Yi et al., 2020). Thus, Td provides a valuable model for studying the parasitic success in a pupal parasitoid and serves as a promising control agent on invasive pests. However, the mechanisms underlying the successful parasitization of Td remains largely unknown.

By conducting an interdisciplinary study that integrates multi-omics analyses and functional behavioural assays, we found that, to adapt to the limited resources of the pupal host, this parasitoid has evolved weaponized venom and teratocyte cells to help arrest host development and speed up the digestion of host tissues. In addition, Td allowed intraspecific competition as a conditional collaboration to compensate for its inability to find more appropriate hosts (the younger ones) but effectively avoided interspecific competition with larval parasitoids. The availability of multi-omics resources and knowledge of parasitism will further benefit the

optimization and utilization of Td in pest management.

Results

Td effectively parasitizes *D. suzukii* and a broad range of drosophilids

Both Td and Aj were trapped in the field and maintained in the laboratory for further study. Aj wasps mainly parasitize 2nd instar *Drosophila* larvae, showing a 60% parasitism rate (the proportion of hosts parasitized) and a 48% emergence rate (the proportion of hosts with wasps hatched) on *D. suzukii*. In comparison to Aj, Td laid eggs in the pupae (Figure 1A) and presented a much better parasitic performance on *D. suzukii*, showing an 85% parasitism rate ($p < 0.001$) and a 77% emergence rate ($p < 0.001$) (Figure 1B and C). To investigate the host range, we tested their parasitic efficiencies in another five *Drosophila* species, including three species in the melanogaster subgroup (*D. melanogaster*, *D. simulans*, and *D. santomea*) and two species outside the melanogaster subgroup (*D. pseudoobscura* and *D. virilis*). Of these hosts, Td showed high parasitism rates in all species (ranging from 80% to 89%) and high emergence rates in most species (ranging from 73% to 79%), except in *D. santomea* (22%) (Figure 1B and C). Aj could also parasitize these drosophilid species but showed much poorer performance in the non-melanogaster subgroup (Figure 1B and C). The parasitism spectrum in the laboratory showed that Td is also a generalist parasitoid with a wide host range, including *D. suzukii* and many other *Drosophila* species.

Td shows a relatively large genome and encodes many copies of tissue inhibitors of

metalloproteinase (*Timp*) genes

Genomic information is critical to characterize the molecular bases underlying parasitic strategies, which is absent for Td. We first sequenced and *de novo* assembled Td reference genome based on PacBio long reads (120.1 Gb). The assembled 938.6 Mb genome consisted of 1633 contigs with an N50 size of 146.9 Mb (Supplementary Table S1). BUSCO estimation showed a high level of completeness (96%) in terms of insect proteins (Supplementary Table S1). By combining 143.7 Gb Hi-C data, 97.8% of assembled contigs were further anchored to six pseudochromosomes, agreeing with the karyotype staining estimation (Figure 1—figure supplement 1).

The assembled Td genome (938.6 Mb) represents an occasionally large one in parasitoids, since most published parasitoid and hymenopteran genomes were relatively small (< 500 Mb) (Figure 1D). Parasitic lifestyle was previously assumed to be associated with reduced genome size and complexity (Moran, 2002; Wicke et al., 2013; Poulin and Randhawa, 2015). While this study was in preparation, Ye *et al*. reported two large genomes (~950 Mb) of *Anastatus* parasitoids (Chalcidoidae) and proposed that the unexpected genome expansion was due to recent bursts of long terminal repeat (LTR) retrotransposons. Similarly, we found recent bursts of transposon elements (TEs) in Td genome (Figure 1E), although a different class of TEs (DNA transposons, rather than LTRs) was the most abundant (Figure 1—figure supplement 2). We further found that the age of the TE burst and the abundance of different classes both highly varied across parasitoid genomes, regardless of the whole genome size (Figure 1D, Figure 1—figure supplement 2). The previous study has also proposed that the expanded genome of *Anastatus* is stabilized owing to the expansion of the *Piwi* gene family (Ye et al., 2022); however, Td genome only encodes three *Piwi*

genes, which is similar to most other Hymenoptera species but much lower than those of *Anastatus* (16 and 30 genes). These patterns suggest that the mechanisms to maintain the stability of genome size may vary between species and that the highly dynamic evolution of repeat contents has shaped great diversity across parasitoid genomes.

By combining *ab initio* gene signatures, transcriptome evidence, and homologue alignments, we generated an official gene set consisting of 16,287 protein-coding genes for Td (Supplementary Table S1; Methods). We used one-to-one orthologous protein genes to infer phylogenetic relationships across representative parasitoids. In Hymenoptera, parasitoidism evolved and underwent massive habitat diversification, including scattered secondary losses (Figure 1D) (Peters et al., 2017; Blaimer et al., 2023; Polaszek et al., 2023). Adaptations to a certain host life stage, i.e. eggs, larvae, or pupae, evolved independently in different sublineages (Figure 1D). Td was placed as a sister sublineage to a large group of chalcid parasitoids with a divergence time of approximately 98 million years ago (Mya) (Fig 1D). Its divergence from *Leptopilina*, another major genus of drosophilid parasitoids (Cynipoidea), dates back 120 Mya (Figure 1D).

Orthologue analysis showed that half of each parasitoid gene set consisted of universal genes across species (Figure 1—figure supplement 3). Interestingly, approximately 83% of universal genes in Td experienced gene duplication events. By sorting all the expanded gene families within and between species, we found that the gene family encoding tissue inhibitors of metalloproteinases (TIMPs; IPR001820) was an extreme outlier (Figure 2A, Supplementary Table S2). Td genome encodes 29 *Timp* genes, much more than that of any other hymenopteran species

(0-7 genes). These copies were located in 10 neighbouring regions of all Td chromosomes and formed three phylogenetic clades unique to Td, indicating multiple recent duplications (Figure 2B and C). Expression profiling of *Timps* showed widespread expression in most copies except for a unique sublineage that showed specialized expression in the venom glands (Figure 2D). These two copies (termed TdTimp1 and TdTimp2) are described below.

Td arrests host development via injection of venom

High-quality, fully annotated genomic resources allowed us to explore the molecular architecture of various adaptive traits of Td. Td is a typical pupal parasitoid that lays eggs exclusively in the pupal stage of hosts; adult wasps emerge from the host pupae after approximately 18 days at 25 ℃ (Figure 1A and Figure 3A). The pupal stage of the hosts is a non-feeding stage that normally lasts no longer than 5 days for *D. suzukii* and *D. melanogaster* at 25 ℃. Thus, pupal parasitoid wasps should have evolved unique strategies to utilize limited nutritional resources effectively during a limited period. One such adaptation is the consequent developmental arrest of the host, which is commonly observed in parasitized hosts (Rivers and Denlinger, 1995; Beckage and Gelman, 2004). We monitored this process in real-time at 24-hour intervals after parasitization of 1-day-old host pupae of *D. suzukii*. Compared to non-parasitized pupae, parasitized pupae showed evident defects in eye pigment deposition and bristle formation (Figure 3B, Figure 3—figure supplement 1A), strongly indicative of developmental arrest. These phenotypic alterations started to occur on the second day post-parasitization (Figure 3B, Figure 3—figure supplement 1A), indicating that the development of the host pupae was immediately stopped after parasitization. We also performed

parasitization experiments on another host species, *D. melanogaster*, for parallel comparisons and in-depth functional genetic investigations. Here, a similar pattern of developmental arrest was observed when *D. melanogaster* pupae were provided for parasitization (Figure 3C, Figure 3—figure supplement 1B).

The most likely effector resulting in host development arrest is the venom, given that parasitoid wasps always inject venom into hosts along with oviposition to condition and manipulate the host for the successful development of wasp progeny (Werren et al., 2010; Asgari and Rivers, 2011; Moreau and Asgari, 2015). To test this hypothesis, the venom fluid from the reservoir of a single Td female was isolated and injected into 1-day host pupae under two levels of dilution (1:20 and 1:40) to monitor host development (Figure 3A). As expected, doses 1:20 and 1:40 markedly delayed the development of both host species in comparison to the control (Figure 3B and C, Figure 3—figure supplement 1). Moreover, the alternating effects of a higher dose of venom (1:20 dilution) were very similar to those parasitized by Td and stronger than those of the lower dose (1:40 dilution). Thus, our results suggest that Td may arrest host development via the coinjection of venom.

Timps are the main venom compounds responsible for host development arrest

To uncover the venom components that confer host developmental arrest, we sequenced the transcriptome of Td venom glands (VGs) and characterized 641 genes with solid expression evidence (Supplementary Table S3). Given that not all expressed genes are necessarily translated and secreted into the reservoir, we performed LC–MS/MS on Td venom to further characterize

reliable venom proteins (VPs) (Supplementary Table S3). Of the 27 highly expressed (Z test, $p < 0.05$) VPs with known functions, a pair of *Timp* genes with the highest expression values attracted the most attention. Surprisingly, these two Timp genes were the previously highlighted *Timp1* and *Timp2* genes that showed expression specialization of venoms from the massive expansion in Td genome (Figure 2).

In insects, matrix metalloproteinases (Mmps) regulate pupal development by degrading extracellular matrix proteins, and Timp delays pupal development (Jia et al., 2017; Jia and Li, 2023). Thus, we wondered whether Td uses these specialized Timps to arrest host development. To test this hypothesis, we mimicked Td parasitization by applying a modified UAS/GAL4 system to drive spatiotemporally specific expression of exogenous *Timp* in *Drosophila* pupae (Figure 3E). As expected, the development of *D. melanogaster* pupae was markedly delayed upon the expression of *DmTimp* (Figure 3F, Figure 3—figure supplement 2 and 3). Although ectopic expression of either *TdTimp1* or *TdTimp2* did not lead to a visible developmental delay, driving the expression of both *TdTimp1* and *TdTimp2* arrested the development of *D. melanogaster* as effectively as the expression of *DmTimp* (Figure 3F, Figure 3—figure supplement 2 and 3). Taken together, these results suggest that cocktails of TdTimp1 and TdTimp2 are bioactive compounds of the venom that result in host development arrest.

Td releases teratocytes to dissociate host tissues

Parasitized wasp larvae feed largely on host fluids for development. We found that as host development was arrested, Td simultaneously released a special group of cells into the host

haemocoel along with egg hatching (Figure 4A, Figure 4—figure supplement 1). Approximately 100 cells were secreted into the host haemocoel after larval hatching (Figure 4—figure supplement 2A). The cell number remained constant during the first three days, then decreased drastically, and finally vanished on day 8 (Figure 4—figure supplement 2A); that is, these cells no longer divided after being released. Moreover, these cells rapidly grew, with initially 85 ± 13 μm in diameter and up to approximately 249 ± 57 μm before vanishment (Figure 4—figure supplement 2B and C). These characteristics agree with those of teratocytes found in other parasitoid sublineages (Hotta et al., 2001; Pedata et al., 2003; Firlej et al., 2007). Thus, we defined these cells as teratocytes, which is the first discovery of teratocytes in the family Diapriidae. Transmission electron microscopy of Td teratocytes revealed a dense lawn of microvilli on the cell surface and that each cell consisted of a spherical nucleus, substantial amounts of rough endoplasmic reticulum, and mitochondria (Figure 4B). These features indicate high levels of protein synthesis and secretory activity in Td teratocytes.

We observed that host tissues started to be digested after the teratocytes were released into the host haemocoel. Do the teratocytes confer the digestion process? We tested this hypothesis by coculturing Td teratocytes and host tissues *in vitro*. Td teratocytes were purified from parasitized hosts and cultured with representative *D. suzukii* tissues, including the brain, testes, and ovaries, in Schneider's medium. Compared with the control, which was maintained for 30 hours without digestion, host tissues incubated with teratocytes from a single parasitoid were partially digested at 12 hours and fully digested after 30 hours (Figure 4C). These findings suggest that teratocytes facilitate the effective dissociation of host tissues, which may play a key role in nutritional

exploitation for parasitoid larvae development.

Teratocytes digest host tissues via trypsins

Although teratocytes have been reported in several other species, their molecular composition remains largely unknown in general (Burke and Strand, 2014; Strand, 2014). We further conducted transcriptomic profiling to characterize the teratocyte genes that facilitate host tissue digestion. A total of 3784 genes were expressed in teratocytes (Supplementary Table S4). The majority of the 129 genes with significantly high expression (Z-test, $p < 0.05$) were ribosome- (48 genes) and digestion-related genes (23 genes) (Figure 4D). Eight trypsin genes dominated among the highly expressed digestion-related genes in teratocytes, indicating their essential role in digesting host tissues.

Trypsin is the most abundant proteinase in invertebrate digestive systems (Muhlia-Almazán et al., 2008; Dias et al., 2015; Shao et al., 2021). To verify their functions in parasitization, trypsin inhibitors (TLCK and TPCK) were added to the incubation system of teratocytes and host tissues (*D. suzukii* testes) to determine whether digestion could be prevented. Along with the increase in inhibitor concentration, we found that the digestion of host tissues was gradually inhibited (Figure 4E, Figure 4—figure supplement 3, Figure 4—figure supplement 4A and B). We then injected trypsin inhibitors directly into the parasitized host pupae to investigate whether this digestion process benefits parasitization. As expected, applying a trypsin inhibitor resulted in significantly lower emergence rates of parasitoid wasps, especially upon the injection of higher amounts of inhibitors (Figure 4F, Figure 4—figure supplement 4C). Correspondingly, we

noticed that the trypsin inhibitor injection led to abnormal wasp larvae development. Upon injection of 400 ng TLCK per host, the parasitoid larvae were found to be significantly smaller than the control on day 4 and almost dead on day 6 post-parasitization, owing to the lack of well-digested food (Figure 4G, Figure 4—figure supplement 5). Altogether, these results suggest that teratocytes degrade host tissues using digestive enzymes, such as trypsin, to provide essential nutrients for the development and survival of wasps. Other digestion-related enzymes may also contribute to host tissue digestion, although their functions deserve further investigation.

Td benefits from parasitizing young host pupae but cannot discriminate between young and old hosts

We showed that Td had evolved the functional integration of arresting host development and digesting host tissues to facilitate the utilization of limited resources in host pupae. In drosophilids, larval structures are lysed during the early pupal period, and adult structures begin to develop during the late period. Thus, Td should parasitize younger host pupae to earn longer developmental times and better nutritional resources. Indeed, the respective functions of venom and teratocytes were tested with the prerequisite of parasitization on newly pupated hosts (Figure 3 and Figure 4). By testing the parasitism efficiency in host pupae of different ages (1- to 4-day-old *D. suzukii* or *D. melanogaster*), we found that Td fed old host pupae (4-day-old) showed a dramatic reduction in both parasitism rate and wasp emergence rate ($p < 0.001$) (Figure 5A and B, Figure 5—figure supplement 1A and B). Simultaneously, both male and female wasps that emerged from young hosts (1-day-old) exhibited larger body sizes than those that emerged from

old pupae (Student's t-test, $p < 0.001$) (Figure 5C, Figure 5—figure supplement 1C). For parasitoids, successful parasitism largely depends on the development of ovaries and VGs in females (Segoli and Rosenheim, 2013; Moreau and Asgari, 2015; Huang et al., 2021). We further found that the ovaries and VGs of females that emerged from young hosts were significantly larger than those from old hosts ($p < 0.001$) (Figure 5D and E, Figure 5—figure supplement 1D and E). By dissecting the ovaries, we found significantly more mature eggs from females that emerged from young host pupae ($p < 0.001$, Figure 5E, Figure 5—figure supplement 1E). These results showed that the parasitization of young hosts benefits the fitness of Td.

The next compelling question was whether Td wasps could recognize host pupae of different ages before parasitization and subsequently prefer to parasitize younger pupae for maximum fitness. Thus, we designed a two-choice oviposition assay and monitored the host selection preferences of Td wasps (Figure 5F). Specifically, 20 young hosts (1-day-old *D. suzukii* or *D. melanogaster* pupae) were attached to the left side of a container, whereas pupae of different ages (1- to 4-day-old) were attached to the right side for competition. Ten Td female wasps (3-day-old) were released into the bottle and allowed to choose the host for oviposition freely (Figure 5F). After a certain time (2 or 4 hours for oviposition choice), the number of eggs laid in the host pupae between the two sides was compared to determine the oviposition preference. Regardless of whether the choice lasted for 2 or 4 hours, Td wasps showed no significant preference for either young or old host pupae (Figure 5G, Figure 5—figure supplement 1F). These results indicate that Td wasps have not evolved the ability to discriminate the young host pupae as a priority for parasitization.

Superparasitism enhances parasitic success in older hosts

The parasitic success of Td largely relies on locating a young host; however, Td does not have the ability to discriminate between young and old hosts. Whether Td has evolved any adaptive strategies to compensate for this disadvantage? We noted that more than one female wasp parasitized the same host in both the laboratory and field (Figure 5—figure supplement 2), leading us to speculate that unexpected superparasitic behaviour (laying more than one egg per host) might be allowed or adaptive in Td. To test this hypothesis, we evaluated the parasitic efficiency of hosts with multiple infections. Strikingly, both the parasitism and emergence rates were significantly improved by superparasitism (Figure 5A and B). The resulting benefit was particularly evident in parasitizing old pupae (4-day-old), in which low parasitic efficiencies by monoparasitism were recovered 2.2-fold (parasitism rate) and 3.2-fold (emergence rate) by superparasitism (Figure 5A and B).

Superparasitism is generally uncommon in solitary parasitoids because only one adult can emerge from the host. Despite the better parasitization performance, we noted that only one adult Td emerged from the superparasitized pupae. Superparasitism likely leads to the additional introduction of venom and teratocytes, which maximizes the utilization of host nutrition, especially in older hosts with poorer resources. Therefore, superparasitism in Td may partially compensate for the inability to recognize young pupae as hosts.

Td avoids interspecific competition with larval parasitoids

Approximately 50 parasitoids have been reported to attack drosophilids (Carton et al., 1986), including larval (e.g. Aj) and pupal parasitoids (e.g. Td). This overlapping ecological niche leads to potential interspecific competition between larval and pupal parasitoids within the same host range. Because Td allows conditional intraspecific competition, the next compelling question would be whether Td allows interspecific competition with larval parasitoids. We provided Td with *D. suzukii* or *D. melanogaster* pupae that had been parasitized by Aj at the larval stage (Figure 6A). We found that Td wasps used their ovipositors to sting Aj-parasitized host pupae, similar to what they did for non-parasitized pupae. However, almost no eggs were laid inside these Aj-parasitized Td-stung pupae, in contrast to the high oviposition rate (approximately 93% for both *Drosophila* hosts) of non-Aj-parasitized pupae (Figure 6B). Thus, Td could discriminate between larva-parasitized hosts to avoid competition with larval parasitoids.

Given that Td wasps use ovipositors to sting both parasitized and non-parasitized pupae before oviposition, we hypothesised that Td ovipositors, in addition to the well-defined function of oviposition, might serve as sensory organs to evaluate the status of host pupae. Td ovipositor is an anatomical and functional cluster consisting of an ovipositor sheath and ovipositor stylet (Figure 6C), of which the unsheathed stylet is more likely to probe and stab. Using scanning electron microscopy, we found that the ovipositor stylet had two types of sensilla on its dorsal and ventral valves: the surface-dome and the coeloconic sensilla (Figure 6D–6I). Coeloconic sensilla was the most abundant type, and secretory pores and surface-dome sensilla were also found on Td ovipositor stylets (Figure 6F–6I). These sensilla and secretory pores occurred on the distal end of the ovipositor stylet but not on the proximal end, and there were more sensilla and secretory pores

on the dorsal valve than on the ventral valve (Figure 6D–6F). These anatomical features support a possible role of the ovipositor stylet in host discrimination.

We sequenced the transcriptome of the ovipositors and made a comprehensive comparison with various Td tissues and organs. Based on the overall expression profiles, principal component analysis placed the ovipositor closer to the antennae and legs of both males and females (Figure 6J), indicating a strong functional correlation among these anatomically non-contact organs. Given that the antennae and legs are well-defined sensory organs for volatile and contact semiochemicals in insects (Vosshall et al., 1999; Schütz et al., 1999; Scott et al., 2001; Kim et al., 2003), respectively, the expression correlation supports the role of oviposition in sensing host environmental signals. By further comparing the expression profiles of ovipositors and female antennae, we found that three chemosensory protein genes (CSPs) and two odourant-binding protein genes (OBPs) showed extremely high expression in both tissues, as well as a few genes encoding gustatory receptors (GRs) and olfactory receptors (ORs) (Figure 6K). More interestingly, the general co-receptor, Orco, which forms heteromultimeric complexes with other ligand-selective ORs, does not express in the ovipositor (Figure 6—figure supplement 1) and most genes related to odourant reception (i.e., OBPs and other ORs) showed biased expression in the antennae, while most taste recognition-related genes, i.e., GRs and CSPs, were more highly expressed in the ovipositor (Figure 6K). Correspondingly, we found a few GRs with the highest expression in ovipositors (Figure 7, Supplementary Table S5). These patterns further support the hypothesis that, unlike the antennae that confer odourant chemoreception, Td ovipositors are more likely to serve as taste organs by sensing contact signals inside the host pupae for host discrimination. How

gustation regulates the senses of other parasitoids requires further investigation.

Discussion

Td has evolved an integrated molecular adaptation for nutrition utilization

Parasitoid wasps are a highly diverse group of insects that are renowned for their diverse life history strategies and co-evolution with their hosts (Pennacchio and Strand, 2006; Harvey et al., 2013; van de Kamp et al., 2018; Ode et al., 2022). Many koinobiont parasitoids that attack early host periods (e.g. larvae) maintain hosts alive and growing for sustained resource availability (Brodeur and Boivin, 2004; Pennacchio and Strand, 2006), while certain idiobiont parasitoids that usually attack non-feeding host stages (e.g. pupae) alternatively arrests host development for high-quality resources. *Drosophila* are natural hosts for multiple parasitic wasps of different genera, including both larval and pupal parasitoids. Their parasitic strategies have been widely studied and reported in multiple parasitoid species, with a particular focus on venom evolution and behavioural adaptations (Mortimer et al., 2013; Martinson et al., 2017; Ramroop et al., 2021; Huang et al., 2021; Chen et al., 2021; Wertheim, 2022). How to conflict with host immune responses and manipulate the host to create a suitable environment are important for larval parasitoids because the hosts are relatively active and proficient in immunity during the larval stage. For example, previous studies have shown that immune suppressors and virulence proteins dominate the VPs of *Leptopilina* larval parasitoids (Colinet et al., 2011; Colinet et al., 2013; Poiri é et al., 2014; Heavner et al., 2017; Huang et al., 2021).

Td is a highly successful pupal parasitoid colonizing a broad range of *Drosophila* species,

including *D. suzukii*. In the present study, we demonstrated the molecular adaptation of Td to achieve parasitic success (Figure 8). Td uses venom to arrest host pupal development and maintain young status via the recruitment of *Timps* (Figure 3). Moreover, Td released a special type of cell along with egg hatching, teratocytes, to accelerate the digestion of host tissues (Figure 4). The functional integration benefits Td as the utilization of nutritional resources is highly efficient during a limited period. The adaptations adopted by pupal parasitoids are largely unique to those of larval parasitoids and highly associated with the non-feeding and relatively inactive conditions of pupae. Correspondingly, few characterized genes of these parasitic effectors were related to immune responses (Supplementary File Tables S3 and S4), indicating that conflict with host immunity plays a minor role in the adaptation of pupal parasitoids.

Another genus of pupal parasitoids, *Nasonia*, that feeds on multiple fly species but not drosophilid flies, has been the subject of genetic, ecological, developmental, and behavioural research for many years (Beukeboom and Desplan, 2003; Werren et al., 2009; Werren et al., 2010), but it serves as a model for specialized investigations of pupal parasitization. Notably, many strategies uncovered in this study have not been described in *Nasonia*, which may advance our understanding of the parasitism of pupae and the utilization of Td as a unique system for studying ecological niche differentiation of parasitoids.

Gene duplication and expression shift play a dominant role in Td functional adaptations

Parasitic effects on organs and tissues provide excellent systems for studying the evolutionary modes of novel genes. Although it was proposed that the co-option of single-copy genes plays a

common role in recruiting venom genes in certain parasitoids, such as *Nasonia* (Martinson et al., 2017), specific cases have also been reported highlighting gene duplication events, including duplicated *Lar* in the venom of a generalist *L. heterotoma* that suppresses host immune responses and the massive expansion of *Warm* in *L. boulardi*, which helps the specialist parasitoid evade host immune attacks (Huang et al., 2021). These differences suggest a highly diverse evolutionary mode of parasitism across different genera. In this study, we characterized Timps as a major compound in the venom that confers host developmental arrest (Figure 3), trypsin as a major component in teratocytes that facilitates host digestion (Figure 4), and a set of chemoreception proteins recruited by ovipositors for taste recognition (Figure 6). Strikingly, all affected genes were found to have undergone massive duplication events.

As described in the genome-wide analysis, *Timp* was the most expanded gene family in Td genome (Figure 2A). By searching for Timps across insects, we found that this gene family was mainly present in holometabolous insects such as Diptera, Lepidoptera, Coleoptera, and Hymenoptera (Figure 2C), possibly because of its role in regulating metamorphosis in this class of insects. The massive expansion of *Timps* in Td was derived from three independent phylogenetic sublineages, including one clustered with other hymenopteran copies, one clustered with patchy copies inside the clade of other insect orders, and one that is relatively unique (Figure 2C). The third sublineage is of the most expansion, in which most components were located on chromosome 6 and showed widespread expression across most tissues and developmental stages (Figure 2B and D). The two VP genes (*TdTimp1* and *TdTimp2*) that confer host development arrest were derived from tandem duplication of this sublineage and further experienced expression

specialization in venom. We noted another four copies of this sublineage that possibly translocated to other chromosomes, showing expression specialization in larvae and teratocytes (Figure 2B and D). Similarly, we found that a few GRs originated from tandem duplications and experienced an expression shift to the ovipositor (Figure 7). Thus, we propose that gene expression, followed by gene expansion, may play a common role in the unique functional adaptations of Td.

Td allows intraspecific competition but refuses interspecific competition from larval parasitoids

Parasitoid wasps are also excellent systems for studying the complex interrelationships within an ecosystem, because their survival and reproduction depend highly on the limited nutrients within a single host (Harvey et al., 2013; Ode et al., 2022). In addition to molecular adaptations, we uncovered ecological adaptations underlying Td parasitism, including the conditional allowance of intraspecific competition and strict refusal of interspecific competition (Figure 8).

Superparasitism usually lowers the reproductive efficiency of parasitoids by affecting their development, resulting in premature mortality of both hosts and parasitoids. Many parasitoid species avoid superparasitism by refusing to lay eggs in their parasitized hosts. For instance, the larval parasitoid *L. boulardi* utilizes EsGAP VPs to trigger parasitized hosts' escape behaviour, resulting in avoiding superparasitism (Chen et al., 2022). However, superparasitism is conditionally allowed if it benefits parasitoids. Despite the evolved molecular adaptations, we found that Td's parasitic success largely depended on its location to a host pupa of the appropriate age (newly pupated) (Figure 5A–5E). However, the ability to discriminate young pupae is

unavailable in Td (Figure 5G). Superparasitism was frequently observed in Td and was further verified by its role in improving parasitic efficiency in old hosts (Figure 5A and B) despite the emergence of only one parasitoid. We hypothesized that the additional introduction of venom and teratocytes by partners within a single host pupa might accelerate the nutritional utilization of pupal parasitoids. Thus, intraspecific competition partially serves as a collaboration that can maximize the survival rate of offspring and favour the population at the cost of individuals.

Interspecific competition is widespread in the highly overlapped ecological niches among parasitoids. Approximately 50 hymenopteran parasitoids have been reported to infect various *Drosophila* species (Carton et al., 1986), including larval parasitoids from Figitidae (e.g., *Leptopilina*) and Braconidae (e.g., Aj) as well as pupal parasitoids from Pteromalidae and Diapriidae (e.g., Td). Except for Pteromalidae parasitoids, most are highly specialized in *Drosophila*. Importantly, larval parasitoids have priority in occupying hosts, imposing strong selection pressure on pupal parasitoids to locate hosts. Unlike intraspecific competition, Td strictly avoided interspecific competition with larval parasitoids. Our results showed that Td effectively recognized and refused to lay eggs in Aj-parasitized hosts (Figure 6). Furthermore, this ability possibly depended on the evolved sensilla on the ovipositor stylet of Td, along with the ability for host discrimination via taste recognition (Figure 6). These uncovered ecological adaptations of Td provide valuable empirical knowledge regarding how organisms deal with inter- and intraspecific competition in nature and how ecological adaptations reconcile with functional innovations.

Insights into the utilization of parasitoids as agents of pest control

In addition to serving as a study system in biology and ecology, parasitoids have been widely used as biological control agents because of their environmental friendliness and ability to suppress pest populations substantially (Smith, 1996; Beckage and Gelman, 2004; Liu et al., 2015). Our study began with identifying a highly successful parasitoid on *D. suzukii* and a broad range of other drosophilids. Although a few larval parasitoid species in Asia, such as Aj, have been reported to successfully parasitize *D. suzukii*, other parasitoids either do not prefer *D. suzukii* or show poor parasitic efficiency on *D. suzukii* (Chabert et al., 2012; Mazzetto et al., 2016; Kremmer et al., 2017). We estimated that the parasitic efficiency of Aj in *D. suzukii* in this study was approximately 50% (Figure 1B and C). In contrast, the great parasitic performance of Td on *D. suzukii* has been observed in this study, indicating the prospective potential of Td utility in the biological control of *D. suzukii.* The molecular and ecological adaptations of Td will provide important knowledge for further improving this potential agent.

Materials and methods

Insects

The strain of pupal parasitoid *T. drosophilae* (Td) trapped from orchards in Hangzhou, Zhejiang, China (30.29 °N, 120.08 °E) in May 2016 was used for experiments (strain Hangzhou), while the strain of larval parasitoid *A. japonica* (Aj) collected from orchards in Taizhou, Zhejiang, China (28.50 °N, 120.34 °E) in June 2018 was used for control parasitization assays (strain Taizhou). The complete mitochondrial genomes of these two strains were sequenced and submitted to GenBank with the accession number MN966974 (Td) and MN882556 (Aj), respectively. The primers for COI sequence amplification of the two wasp species were provided in Supplementary Table S6. Both strains were developed from an individual mother and maintained on *D. melanogaster* strain *Canton-S* in the laboratory. Td was allowed to parasitize *Drosophila* pupae, and Aj was allowed to parasitize 2nd instar *Drosophila* larvae. The infected hosts were maintained at 25 ℃ until adult wasps emerged. The newly emerged wasps were collected into vials containing apple juice agar medium until exposure to hosts. The apple juice agar recipe was 27 g agar, 33 g brown sugar and 330 ml pure apple juice in 1000 ml diluted water.

D. melanogaster Canton-S (#BL64349) and *UAS-Timp* (#BL58707) lines were acquired from the Bloomington Drosophila Stock Center. The ubiquitous driver *da-GAL4* (#TB00103) line was acquired from the Tsing Hua Fly Center. *D. simulans* (#BCF93), *D. pseudoobscura* (#BCF95) and *D. virilis* (#BCF97) were acquired from the Core Facility of *Drosophila* Resource and Technology, Chinese Academy of Sciences. *D. suzukii* (Strain Hangzhou) was collected in the above traps with their parasitoid wasps, and its mitochondrial genome accession number in

GenBank is MW237837.1. *D. santomea* was provided by Dr. Qi Zhou (Zhejiang University, China).

To generate *UAS-TdTimp1* and *UAS-TdTimp2* transgenic flies, the coding regions of *TdTimp1* and *TdTimp2* were amplified from the cDNA of Td wasps using the primers listed in Supplementary Table S6. The resulting cDNA fragment was digested with NotI (NEB, USA) and EcoRI (NEB, USA) and inserted into the pUAST-attB vector. The plasmids of *TdTimp1* and *TdTimp2* were injected into *Drosophila* embryos and integrated into the *attP* sites on chromosome 2 (cytological loci 25C6) and chromosome 3 (cytological loci 86F8), respectively.

Genome sequencing

Td samples for genome sequencing have been maintained in the laboratory for at least 50 generations. To generate a high-quality chromosome-level genome, Td genome was fully sequenced using long-read sequencing technology (PacBio) and Hi-C. For PacBio sequencing, DNA was extracted from a pool of ~1000 male Td adults of a monoisolate to meet the requirements for library construction using a DNeasy Blood and Tissue Kit (Qiagen, Germany). DNA quality was checked using gel electrophoresis (0.8% agarose gel) and a High Sensitivity DNA Kit (Agilent, USA) in combination with a Bioanalyzer 2100 (Agilent, USA). A 20-Kb genomic library was constructed and sequenced by Berry Genomics Co., Ltd. (Beijing, China) according to the standard protocols on a PacBio Sequel platform. A total of 120.1 Gb raw reads were generated, accounting for 128x genome coverage. This DNA sample was also sequenced using the Illumina platform to yield 57.7 Gb (~61.5X coverage) short reads for the purpose of error correction.

Hi-C libraries were constructed from a pool of 20 newly emerged Td males according to the method previously described in Lieberman-Aiden *et al* (Lieberman-Aiden et al., 2009). Briefly, the samples were fixed with 2% formaldehyde for 10 min at room temperature. Then, glycine solution was added to a final concentration of 100 mM to stop cross-linking. The cross-linked DNA was extracted and digested with HindIII (NEB, USA) overnight. Biotin-14-dCTP17 was introduced during the sticky end repair process. The interacting DNA fragments were ligated to form chimeric junctions using T4 DNA ligase. Finally, Hi-C library sequencing was performed by GrandOmics Co., Ltd. (Wuhan, China) on an Illumina HiseqX Ten platform (Illumina, HiseqX Ten, USA), generating a total of 143.7 Gb paired-end reads (2 × 150 bp), accounting for 153x coverage.

Chromosome staining

Chromosome preparation of Td wasp for karyology was carried out according to the method by Imai *et al.* with some modifications (Imai et al., 1988). Briefly, the cerebral ganglia of both male and female Td early pupae were dissected in Ringer's saline solution under a stereoscope (Leica, Germany) and washed for 3-5 min in Ringer's buffer. The cerebral ganglia were then incubated with 0.005% colchicine-hypotonic solution (diluted in 1% sodium citrate) for 1 h and transferred onto a clean slide. The tissues were fixed in fixative solution A (anhydrous ethanol: glacial acetic acid: double-distilled water at 3: 3: 4 by volume), then the samples were gently broken up with forceps to fully distribute the chromosomes. Finally, the samples were fixed in fixative solution B (anhydrous ethanol: glacial acetic acid at 1: 1 by volume) and mounted in ProLong Gold Antifade Mountant with DAPI (Invitrogen, USA). Fluorescence images were captured on an LSM 800

confocal microscope (Zeiss, Germany).

Genome assembly

PacBio reads were used to assemble contigs using Nextdenovo v2.4.0 (https://github.com/Nextomics/NextDenovo) with the parameters “read_type=clr read_cutof =2k genome_size=900 m seed_depth=60 nextgraph_options=-a 1 -A”. Assembled contigs were corrected and polished using high coverage of Illumina paired-end reads using Nextpolish v1.3.1 (Hu et al., 2020) with the following parameters: “task=best rerun=3 sgs_options=-max_depth 100 -bwa lgs_options=-min_read_len 1k -max_depth 100 lgs_minimap2_options=-x map-pb”. The polished contigs were then subjected to removal of redundancy using purge_dups v1.2.3 (Guan et al., 2020) for two rounds with default parameters.

To realize a chromosomal-level assembly, assembled contigs were further clustered based on Hi-C contact information from Hi-C sequencing reads. Juicer v1.5.7 (Capurso et al., 2020) was used to process the contact signals that were provided for 3d-dna v190716 for chromosome grouping with the parameters “-q 1 --editor-repeat-coverage 2”.

The completeness of the genome assembly was estimated using the BUSCO pipeline v5.4.3 (Waterhouse et al., 2018; Seppey et al., 2019) against insect_odb10.

Transcriptome sequencing and analysis

Td transcriptomes of different developmental stages were obtained from Zhou *et al*. (Zhou et al., 2019), including egg, L1 (Days 1-2 larvae, early larval stage), L2 (Days 3-4 larvae, middle larval stage), L3 (Days 5-6 larvae, late larval stage), P1 (Days 1-3 pupae, early pupal stage), P2 (Days 4-6 pupae, middle pupal stage), P3 (Days 7-9 pupae, late pupal stage), AM (Day 1 male adults) and

AF (Day 1 female adults). The other Td samples for transcriptome analysis included 4-day-old teratocytes, VGs of Day 3-5 AF wasps, and the different parts of Day 3-5 AF and AM Td wasps, including antenna, head without antenna, legs, thorax without legs, ovipositor, and abdomen without ovipositor. All samples were dissected in Ringer's saline solution on an ice plate under a stereoscope (Leica, Germany). Total RNA was independently extracted from each sample using the RNeasy MiniKit (Qiagen, Germany). Construction of the cDNA library and paired-end RNAseq (Illumina, NovaSeq 6000, USA) were carried out by Berry Genomics Co. Ltd. (Beijing, China). Statistics of transcriptome sequencing data are listed in Supplementary Table S7. Each sample was independently mapped to the reference genome using HISAT2 v2.0.5 (Kim et al., 2015) using default parameters. The mapping results were processed using SAMTOOLS v1.9 (Li et al., 2009) as inputs for genome annotation.

We also sequenced full-length transcripts using the PacBio sequencing system (Pacific Biosciences, USA) for genome annotation. A total of 67.4 Gb transcriptome sequencing data of Td were generated from a library with an insert of 1–10 kb for the messenger RNA (mRNA) pool of all stages of Td development (Supplementary Table S7). Raw reads were processed using isoseq v3.2.2 and mapped to the reference genome using minimap v2.1 (Li, 2018) with parameters of "-ax splice -uf --secondary=no -C5".

Genome annotation

Repeat contents were annotated using the pipeline of RepeatMasker (www.repeatmasker.org/RepeatMasker/). Firstly, a Td-specific repeat library was generated using RepeatModeler v2.0.2 (www.repeatmasker.org/RepeatModeler/). RepeatMasker v4.1.1 was then

used to mask the repeat contents across the whole genome against both the Td-specific library and Dfam v3.2 (Storer et al., 2021). Protein-coding genes were predicted based on repeat-masked genome. Multiple gene prediction approaches were used to generate several gene sets, including 1) BRAKER v2.1.5 (Brůna et al., 2021) was applied to predict two gene sets on respectively transcriptome-based hints and related proteins-based hints; 2) Maker v2.31.10 (Holt and Yandell, 2011) was used to predict a gene set by calling SNAP v2006-07-28 (Korf, 2004) and Augustus v3.3.2 (Stanke et al., 2008) and integrating evidence of related proteins and full-length transcripts; 3) StringTie v2.0 (Pertea et al., 2015) was used to combine all Illumina-based transcriptome data to generate a merged transcript set using default parameters; 4) the python module "collapse_isoforms_by_sam" of TOFU (github.com/Magdoll/cDNA_Cupcake) was used to generate a full-length reads-based transcript set, with parameters of "--dun-merge-5-shorter -c 0.9 -i 0.9". All above independent gene sets were subject for pairwise comparisons at both transcript-level and exon-level and retained the consistent ones with the first priority and the ones with multiple lines of supports as the secondary priority. The ones with only support from a single set were excluded. The predicted genes were then annotated with functions based on both BLASTP v2.2.26 against NR databases and a local InterProScan search (v5.38-76.0) (Jones et al., 2014) for domains. Expression values of each gene in each developmental stage or tissue were estimated as TPM using salmon v0.12.0 (Patro et al., 2017) with parameters of "quant -l A". The expression of a specific gene in a given sample was determined based on the threshold value of N99, i.e. the value accounting for 99% of summarized transcripts in the corresponding sample.

Evolutionary analyses

Orthologs across 14 hymenopteran species were sorted using OrthoFinder v2.5.4 (Emms and Kelly, 2019) with parameters "-S blast -M msa". Orthologs with strict single copy in all 14 species were isolated to infer the phylogeny across species and concatenated to a super gene for each species. MAFFT v7.470 (Katoh et al., 2002) was used to perform multiple alignment and extracted with conserved regions by trimAI v1.4.rev15 (Capella-Gutiérrez et al., 2009). The phylogenetic tree was inferred using RAxML v8.2.12 (Stamatakis, 2014) with parameters "-f a -x 12345 -p 12345 -# 100 -m PROTGAMMAJTTF". The tree was illustrated and annotated using iTOL v6.6 (Letunic and Bork, 2021).

Timp homologs in other species were retrieved from the database of InterPro (www.ebi.ac.uk/interpro) based on the domain IPR001820. All 198 insect genes encoding this domain were retrieved and used for phylogenetic analyses as described above.

Venom preparation and microinjection

The venom reservoirs of Td female wasps aged 3 to 5 days were dissected in Ringer's saline solution on an ice plate under a stereoscope (Leica, Germany). The venom reservoirs were washed at least 3 times in Ringer's buffer and placed into a 500 μl screw-top tube. The tube was then mixed with grinding glass beads with a size of 0.5 mm (Tansoole, China) and shaken on a vortex mixer six times for 10 s each time. After centrifugation at 10000 ×g at 4 ℃ for 5 min, the supernatant (venom fluid) was collected and quantified with the BCA Protein Assay Kit (Invitrogen, USA). Approximately 1: 20 (16.2 ng) or 1: 40 (8.1 ng) amounts of the total venom extract derived from a single female wasp were injected into each *D. melanogaster* and *D. suzukii* host pupa using the Eppendorf FemtoJet 4i device with the following parameters: injection

pressure = 900 hPa; injection time = 0.15 s.

Identification of Td venom proteins

For LC–MS/MS experiments, venom fluid from approximately 2000 Td female wasps aged 3 to 5 days was dissolved in 100 μl SDT lysis buffer (4% SDS, 100 mM Tris-HCl, 1 mM DTT, pH 7.6). The sample was boiled for 15 min and then centrifuged at 13,000 × g at 4 ℃ for 40 min. The detergent and DTT were removed with repeated ultrafiltration (Microcon units) using UA buffer (8 M urea, 150 mM Tris-HCl, pH 8.0). Then 100 μl 50 mM iodoacetamide was added to block reduced cysteine residues, and the samples were incubated for 30 min in the dark. Then, the protein suspensions were digested with 3 μg trypsin (Promega, USA) in 40 μl 100 mM NH_4HCO3 buffer overnight at 37 ℃, and the resulting peptides were desalted on C18 cartridges (Sigma, Germany), concentrated by vacuum centrifugation, and reconstituted in 40 μL of 0.1% (v/v) formic acid solution.

LC–MS/MS analysis was performed on a Q Exactive mass spectrometer (Thermo Fisher Scientific, USA) coupled to an Easy nLC HPLC liquid system (Thermo Fisher Scientific, USA). Briefly, 5 μg of the peptide mixture was loaded onto a reverse-phase trap column (Thermo Fisher Scientific Acclaim PepMap 100, 100 μm × 2 cm, nanoViper C18) connected to the C18 reversed-phase analytical column (Thermo Fisher Scientific Easy Column, 10-cm long, 75-μm inner diameter, 3 μm resin) in buffer A (0.1% formic acid) and separated with a linear gradient of buffer B (84% acetonitrile and 0.1% formic acid) at a flow rate of 300 nl/min. The eluted peptides were ionized, and the full MS spectrum (from m/z 300 to 1800) was acquired by precursor ion scan using the Orbitrap analyser with a resolution of r = 70,000 at m/z 200, followed by 20 MS/MS

events in the Orbitrap analyser with a resolution of r = 17,500 at m/z 200. The MS raw files were translated into mgf files and searched against the transcriptome of Td venom gland using Mascot 2.2 (Perkins et al., 1999). MS/MS tolerance was set at 20 ppm, and trypsin was defined as the cleavage enzyme allowing no more than two missed cleavages. Carbamidomethylation of cysteine was specified as a fixed modification, and oxidation of methionine was specified as a variable modification.

Venom-protein genes were finally defined based on both transcriptomic and proteomic evidence as described above. Genes with TPM higher than 16.55 (N99 value) in the venom were defined as venom gland-expressed genes. VG-expressed genes that could be fully aligned to at least three proteomic peptides were defined as venom proteins (Supplementary Table S3). A Z test was performed to define significantly high expression ($p < 0.05$).

Ectopic overexpression of *Timps* in host pupae

To investigate whether ectopic expression of *DmTimp* and *TdTimp* could impair host development, we used a temperature-sensitive conditional GAL4/GAL80^{ts} system to drive UAS-Timp expression only in host pupae (Suster et al., 2004; Caygill and Brand, 2016). Briefly, flies with different transgenic elements were raised at 18 ℃ to suppress da-GAL4 (a ubiquitous expression driver) activity during egg and larva developmental stages. After pupation, the 1-day *Drosophila* pupae were switched to 29 ℃ to inactive GAL80^{ts} activity and thereby permit GAL4 activation of DmTimp and TdTimp, respectively.

Host developmental status observation

The development of *D. melanogaster* and *D. suzukii* pupae was monitored using a stereoscope

(Olympus MVX10, Japan) with a digital microscope camera (Olympus Dp47, Japan), and photos were taken at 24 h intervals. The flies were removed from their pupal case and their eye colours were divided into 5 levels from white (young) to red (old), including white, light orange, orange, light red, and red. The number of flies with different eye colours was counted to measure the developmental effect. All these animals were pupae (after head eversion). The outline around each representative image in Figure 3B, 3C, 3F and Figure 3—figure supplement 2 refers to the pupa case.

Parasitoid body, venom gland and venom reservoir size measurement

Images of the whole body, venom gland and venom reservoir of newly emerged Td from male pupae of *D. melanogaster* and *D. suzukii* of different ages were taken under a microscope (Olympus SZX16, Japan) with a digital camera (FluoCa Scientific, BioHD-C16, Singapore). The length and sizes of the venom gland and venom reservoir were measured by using Scopelmage9.0 software (Bioimager, Switzerland).

Teratocyte number and size measurement

After parasitization by Td, the *Drosophila* hosts at different days post parasitization were dissected in Ringer's saline solution on an ice plate under a stereoscope (Leica, Germany). The number of teratocytes in each host was directly counted. In addition, teratocytes were imaged under a microscope (Olympus SZX16, Japan) with a digital camera (FluoCa Scientific, BioHD-C16, Singapore). The diameters of teratocytes were measured by using Scopelmage9.0 software (Bioimager, Switzerland).

Scanning and transmission electron microscope analyses

For transmission electron microscopy analyses, Td teratocytes were fixed with 2.5% glutaraldehyde in phosphate buffered saline (PBS, 0.1 M, pH 7.2) for 24 h at 4 ℃. Samples were washed three times in PBS for 15 min each and then postfixed in 1% OsO4 for 2 h at 4 ℃. Then, the samples were washed three times in PBS for 15 min each and dehydrated through a graded series of ethanol (30%, 50%, 70%, 80%, 90% and 95% for 15 min each; 100% for 20 min each) and acetone (100%) twice for 20 min. Next, the samples were infiltrated successively with a graded mixture of acetone and Spurr resin (1: 1 for 1 h, 1: 3 for 3 h) and Spurr resin (SPI-Chem, USA) for 12 h at room temperature. Finally, the samples were embedded in Spurr resin and polymerized at 70 ℃ for 12 h. Ultrathin sections (~70 nm) were cut on an ultramicrotome (Leica EM UC7, Germany). The sections were stained with uranyl acetate and lead citrate and were observed and photographed using a transmission electron microscope (Hitachi, H-7650, Japan) operated at 80 kV.

For scanning electron microscope analyses, Td ovipositors were fixed with 2.5% glutaraldehyde in PBS for 24 h at 4 ℃. Samples were washed three times in PBS for 15 min each. Then, samples were postfixed with 1% OsO4 in PBS for 2 h and washed three times in PBS for 15 min each. The fixed samples were dehydrated through a graded series of ethanol (30%, 50%, 70%, 80%, 90% and 95%) for 15 min each and were then placed in absolute (100%) alcohol for 20 min. Samples were vacuum-dried and coated with gold-palladium using an Ion Sputter (Hitachi, E-1010, Japan) and observed with a scanning electron microscope (Hitachi, SU-8010, Japan) operated at 3 kV.

Coculture of teratocytes with host tissues

Teratocytes were dissected from each host 4 days post parasitization and were collected in cell culture dishes containing 3 μl Schneider's *Drosophila* medium (Thermo Fisher Scientific, USA) plus antibiotics (ampicillin and kanamycin, each at a concentration of 100 μg/l). Then, the brain and the pair of testes and ovaries of *D. suzukii* host pupae were dissected. One single tissue was cocultured with teratocytes derived from a single host in Schneider's medium at room temperature. The status of the host tissues was recorded by a stereoscope (Olympus MVX10, Japan) with a digital microscope camera (Olympus Dp47, Japan) after 0 h, 12 h and 30 h of incubation.

Coculture of trypsin inhibitors *in vitro*

Pairs of *D. suzukii* testes were dissected and individually cocultured with teratocytes derived from a single host in Schneider's medium. Two trypsin inhibitors, TLCK (tosyl-L-lysyl-chloromethane hydrochloride) (Sigma, Germany), were added at different concentrations of 0 mM (CK), 0.01 mM, 0.1 mM, and 1 mM; TPCK (L-chloromethyl (2-phenyl-1-(p-toluenesulfonylamino) ethyl) ketone) (Sigma, Germany) was added at different concentrations of 0 mM (CK), 0.005 mM, 0.05 mM, and 0.5 mM. The status of the host tissues was recorded by a stereoscope (Olympus MVX10, Japan) with a digital microscope camera (Olympus Dp47, Japan) after 0 h and 30 h of incubation.

Microinjection of trypsin inhibitors *in vivo*

One-day-old *D. suzukii* pupae were parasitized by Td, and different amounts of TLCK (20 ng, 200 ng, and 400 ng) and TPCK (10 ng, 100 ng and 200 ng) were injected into each host 48 h post infection. We first used tweezers to make a hole at the abdomen of host pupal case, and the microinjection was done through the holes. The microinjection was conducted using the Eppendorf FemtoJet 4i device with the following parameters: injection pressure = 900 hPa;

injection time = 0.15 s. Based on the volume of *D. suzukii* pupa, the approximate concentrations of TLCK were 0.04 mM (20 ng), 0.4 mM (200 ng), and 0.8 mM (400 ng), and the approximate concentrations of TPCK were 0.02 mM (10 ng), 0.2 mM (100 ng), and 0.4 mM (200 ng). The developmental status of wasp larvae was observed in the inhibitor-injected hosts 96 h and 144 h post infection.

Parasitic efficiency assay

For parasitic efficiency assays in Figures 1B and 1C, 3-day-old mated Td females were allowed to parasitize host pupae of different *Drosophila* species at a parasite/host ratio of 1: 10 for 3 h. In addition, 3-day-old mated Aj females were allowed to parasitize 2nd instar host larvae of different *Drosophila* species at a parasite/host ratio of 1: 10 for 2 h. The parasitized hosts were maintained at 25 ℃ for analysis of parasitism efficiency.

For parasitic efficiency assays in Figures 5A and B, Figure 5—figure supplement 1 A and B, Td females were allowed to parasitize different aged (e.g., 1-day, 2-day, 3-day and 4-day-old) pupae of *D. melanogaster* and *D. suzukii*. We then selected hosts with monoparasitism and superparasitism for analysis of parasitism efficiency. Here, monoparasitism indicates that the host pupae were parasitized by Td one time; superparasitism indicates that the host pupae were parasitized by Td $\geq$ 2 times.

The parasitism rate and wasp emergence rate were calculated using the following formulas: Parasitism rate = (1 − number of emerged host adults/number of total hosts) × 100%; Wasp emergence rate = (number of emerged wasps/number of total hosts) × 100%.

Oviposition choice assay

Oviposition choice assays were carried out in a 2.5 × 9.5 cm cylindrical tube (FigURE 5F). Briefly, twenty 1-day-old host pupae were sticky on the left side of the tube, and the same number of X-day-old host pupae (X = 1, 2, 3, or 4) were sticky on the right side. Then, ten 3-day-old Td females were released into the apparatus for performing a 2 h or 4 h egg-laying choice assay. The tested hosts were dissected, and the total numbers of wasp eggs on both sides were counted. The oviposition preference indices (%) were calculated as $(N_1 - N_x)/(N_1 + N_x) \times 100\%$, where N_1 is the total number of wasp eggs in host pupae on the left side and N_x is the total number of wasp eggs in host pupae on the right.

Interspecific competition assay

Three-day-old Aj female wasps were allowed to parasitize 2nd instar larvae of *D. melanogaster* and *D. suzukii*, respectively. The infected hosts were maintained at 25 ℃ until pupation. Then, Aj-parasitized host pupae and regular pupae were provided to 3-day-old Td female wasps. Immediately, Td females used their ovipositor to sting the host pupae. Approximately thirty stabbed Aj-parasitized or regular host pupae were randomly selected and dissected under a microscope, and the portion of the oviposition rate of Td was calculated as the percentage that contained Td wasp egg(s) relative to the total number of hosts that were dissected. At least five replicates were performed for each group.

Quantitative real-time PCR

Total RNA was extracted from different Td tissues (e.g., head, antenna, and so on) using the RNeasy Mini Kit (Qiagen, Germany) and then reverse transcribed into cDNA using HiScript III RT SuperMix for qPCR (Vazyme, China) following the manufacturer's protocol. qRT-PCR was

performed in the AriaMx real-time PCR system (Agilent Technologies, USA) with the ChamQ SYBR qPCR Master Mix Kit (Vazyme, China) using the following temperature cycling conditions: 30 s at 95 ℃, followed by 45 cycles of three-step PCR for 10 s at 95 ℃, 20 s at 55 ℃, and 20 s at 72 ℃. The RNA levels of the target genes were normalized to that of *tubulin* mRNA, and the relative concentration was determined using the $2^{-\Delta\Delta Ct}$ method. All primers used for qRT-PCR in this study are listed in Supplementary Table S6.

Statistics

All statistical analyses were performed in GraphPad Prism version 8.0 (GraphPad Software, USA) and SPSS 26 (IBM, USA). Normal distribution of the data was tested using the Shapiro-Wilk test. The Bartlett chi-square test was used to test the homogeneity of variance of the data, which was consistent with the normal distribution. We used two-tailed unpaired Student's t tests to determine the statistical significance of a difference between two treatments when a parametric test was appropriate. We used the Mann-Whitney U test and Wilcoxon signed rank test for experiments requiring a nonparametric statistical test. ANOVA with Sidak's multiple comparisons tests were used to compare mean differences between multiple groups when a parametric test was appropriate. Fisher's exact test was used to compare the proportion of red eye host pupae and host tissue full digestion. Details of the statistical analysis are provided in the figure legends, including how significance was defined and the statistical methods used. Data represent the mean ± standard error of the mean (SEM). Different letters indicate statistically significant differences ($p < 0.05$). For all other tests, significance values are indicated as *, $p < 0.05$; **, $p < 0.01$; ***, $p < 0.001$.

Data availability

The genomic data and associated transcriptome data are available in NCBI GenBank under BioProject numbers PRJNA922326. The MS proteome data were deposited to the ProteomeXchange Consortium (http://proteomecentral.proteomexchange.org) through the PRIDE partner repository (https://www.ebi.ac.uk/pride/) with the dataset identifier PXD038251. Other datasets generated during and/or analysed during the current study are available from the corresponding author on reasonable request.

Funding

This study was supported by the Natural Science Foundation of China (Grants # 32325044, 32021001, 32302426, 32202375, 32225008), Chinese Academy of Sciences (XDB27040205 and XDPB16), and the Zhejiang Provincial Natural Science Foundation of China (LZ23C140003).

Competing interests

The authors declare that they have no competing interests.

Acknowledgements

We thank Bloomington Drosophila Stock Center, Tsing Hua Fly Center, Shanghai Core Facility of *Drosophila* Resource and Technology, Dr. Qi Zhou for providing *Drosophila* stocks. We also thank Bio-ultrastructure analysis Lab of Analysis center of Agrobiology and environmental sciences, Zhejiang University for providing Scanning and transmission electron microscope

sample preparation and observation platform.

Author contributions

Lan Pang, Data curation, Formal analysis, Investigation, Project administration, Resources, Visualization, Writing – original draft; Gangqi Fang, Data curation, Formal analysis, Investigation, Project administration, Resources, Visualization, Writing – original draft; Zhiguo Liu, Formal analysis, Resources; Zhi Dong, Formal analysis, Resources; Jiani Chen, Visualization; Ting Feng, Investigation; Qichao Zhang, Investigation; Yifeng Sheng, Methodology; Yueqi Lu, Methodology; Ying Wang, Methodology; Yixiang Zhang, Resources; Guiyun Li, Resources; Xuexin Chen, Funding acquisition; Shuai Zhan, Funding acquisition, Supervision, Conceptualization, Writing – original draft, Writing – review & editing; Jianhua Huang, Funding acquisition, Supervision, Conceptualization, Writing – original draft, Writing – review & editing.

References

Asgari S, Rivers DB. 2011. Venom proteins from endoparasitoid wasps and their role in host-parasite interactions. *Annu Rev Entomol* **56**:313–335. DOI: https://doi.org/10.1146/annurev-ento-120709-144849

Asplen MK, Anfora G, Biondi A, Choi DS, Chu D, Daane KM, Gibert P, Gutierrez AP, Hoelmer KA, Hutchison WD, Isaacs R, Jiang ZL, Kárpáti Z, Kimura MT, Pascual M, Philips CR, Plantamp C, Ponti L, Vétek G, Vogt H, Walton VM, Yu Y, Zappalà L, Desneux N. 2015. Invasion biology of spotted wing *Drosophila* (*Drosophila suzukii*): a global perspective and

future priorities. *J Pest Sci* **88**:469–494. DOI: DOI: https://doi.org/10.1007/s10340-015-0681-z

Beckage NE, Gelman DB. 2004. Wasp parasitoid disruption of host development: implications for new biologically based strategies for insect control. *Annu Rev Entomol* **49**:299–330. DOI: https://doi.org/10.1146/annurev.ento.49.061802.123324

Beukeboom L, Desplan C. 2003. Nasonia. *Curr Biol* **13**:R860. DOI: https://doi.org/10.1016/j.cub.2003.10.042

Blaimer BB, Santos BF, Cruaud A, Gates MW, Kula RR, Mikó I, Rasplus JY, Smith DR, Talamas EJ, Brady SG, Buffington ML. 2023. Key innovations and the diversification of Hymenoptera. *Nat Commun* **14**:1212. DOI: https://doi.org/10.1038/s41467-023-36868-4

Boughdad A, Haddi K, El Bouazzati A, Nassiri A, Tahiri A, El Anbri C, Eddaya T, Zaid A, Biondi A. 2021. First record of the invasive spotted wing *Drosophila* infesting berry crops in Africa. *J Pest Sci* **94**:261–271. DOI: https://doi.org/10.1007/s10340-020-01280-0

Brodeur J, Boivin G. 2004. Functional ecology of immature parasitoids. *Annu Rev Entomol* **49**:27–49. DOI: https://doi.org/10.1146/annurev.ento.49.061703.153618

Brůna T, Hoff KJ, Lomsadze A, Stanke M, Borodovsky M. 2021. BRAKER2: automatic eukaryotic genome annotation with GeneMark-EP+ and AUGUSTUS supported by a protein database. *NAR Genom Bioinform* **3**:lqaa108. DOI: https://doi.org/10.1093/nargab/lqaa108

Burke GR, Strand MR. 2014. Systematic analysis of a wasp parasitism arsenal. *Mol Ecol* **23**:890–901. DOI: https://doi.org/10.1111/mec.12648

Capella-Gutiérrez S, Silla-Martínez JM, Gabaldón T. 2009. trimAl: a tool for automated alignment

trimming in large-scale phylogenetic analyses. *Bioinformatics* **25**:1972–1973. DOI: https://doi.org/10.1093/bioinformatics/btp348

Capurso D, Tang Z, Ruan Y. 2020. Methods for comparative ChIA-PET and Hi-C data analysis. *Methods* **170**:69–74. DOI: https://doi.org/10.1016/j.ymeth.2019.09.019

Carton Y, Bouletreau M, van Alphen JJM, van Lenteren JC. 1986. The *Drosophila* parasitic wasps. In: Ashburner M, Carson HL, Thompson JN, editors. The genetics and biology of *Drosophila*. *Springer* pp: 347–394.

Caygill EE, Brand AH. 2016. The GAL4 System: A versatile system for the manipulation and analysis of gene expression. *Methods Mol Biol* **1478**:33–52. DOI: https://doi.org/10.1007/978-1-4939-6371-3_2

Chabert S, Allemand R, Poyet M, Eslin P, Gibert P. 2012. Ability of European parasitoids (Hymenoptera) to control a new invasive Asiatic pest, *Drosophila suzukii*. *Biological Control* **63**:40–47. DOI: https://doi.org/10.1016/j.biocontrol.2012.05.005

Charnov EL. 1994. Parasitoids and darwinian theory parasitoids: behavioral and evolutionary ecology. H. C. J. Godfray. *The Quarterly Review of Biology* **69**:73–76. DOI: https://doi.org/10.1086/418435.

Chen J, Fang G, Pang L, Sheng Y, Zhang Q, Zhou Y, Zhou S, Lu Y, Liu Z, Zhang Y, Li G, Shi M, Chen X, Zhan S, Huang J. 2021. Neofunctionalization of an ancient domain allows parasites to avoid intraspecific competition by manipulating host behaviour. *Nat Commun* **12**:5489. DOI: https://doi.org/10.1038/s41467-021-25727-9

Colinet D, Cazes D, Belghazi M, Gatti JL, Poiri é M. 2011. Extracellular superoxide dismutase in

insects: characterization, function, and interspecific variation in parasitoid wasp venom. *J Biol Chem* **286**:40110–40121. DOI: https://doi.org/10.1074/jbc.M111.288845

Colinet D, Mathé-Hubert H, Allemand R, Gatti JL, Poirié M. 2013. Variability of venom components in immune suppressive parasitoid wasps: from a phylogenetic to a population approach. *J Insect Physiol* **59**:205–212. DOI: https://doi.org/10.1016/j.jinsphys.2012.10.013

Colinet D, Schmitz A, Depoix D, Crochard D, Poirié M. 2007. Convergent use of RhoGAP toxins by eukaryotic parasites and bacterial pathogens. *PLoS Pathog* **3**:e203. DOI: https://doi.org/10.1371/journal.ppat.0030203

Deprá M, Poppe JL, Schmitz HJ, De Toni DC, Valente VLS. 2014. The first records of the invasive pest *Drosophila suzukii* in the South American continent. *J Pest Sci* **87**:379–383. DOI: https://doi.org/10.1007/s10340-014-0591-5

Dias RO, Via A, Brandão MM, Tramontano A, Silva-Filho MC. 2015. Digestive peptidase evolution in holometabolous insects led to a divergent group of enzymes in Lepidoptera. *Insect Biochem Mol Biol* **58**:1–11. DOI: https://doi.org/10.1016/j.ibmb.2014.12.009

Dos Santos LA, Mendes MF, Krüger AP, Blauth ML, Gottschalk MS, Garcia FRM. 2017. Global potential distribution of *Drosophila suzukii* (Diptera, Drosophilidae). *PLoS One* **12**:e0174318. DOI: https://doi.org/10.1371/journal.pone.0174318

Emms DM, Kelly S. 2019. OrthoFinder: phylogenetic orthology inference for comparative genomics. *Genome Biol* **20**:238. DOI: https://doi.org/10.1186/s13059-019-1832-y

Firlej A, Lucas É, Coderre D, Boivin G. 2007. Teratocytes growth pattern reflects host suitability in a host-parasitoid assemblage. *Physiol Entomol* **32**:181–187. DOI:

https://doi.org/10.1111/j.1365-3032.2006.00548.x

Gasmi L, Sieminska E, Okuno S, Ohta R, Coutu C, Vatanparast M, Harris S, Baldwin D, Hegedus DD, Theilmann DA, Kida A, Kawabata M, Sagawa S, Takatsuka J, Tateishi K, Watanabe K, Inoue MN, Kunimi Y, Kim Y, Erlandson MA, Herrero S, Nakai M. 2021. Horizontally transmitted parasitoid killing factor shapes insect defense to parasitoids. *Science* **373**:535–541. DOI: https://doi.org/10.1126/science.abb6396

Guan D, McCarthy SA, Wood J, Howe K, Wang Y, Durbin R. 2020. Identifying and removing haplotypic duplication in primary genome assemblies. *Bioinformatics* **36**:2896–2898. DOI: https://doi.org/10.1093/bioinformatics/btaa025

Harvey JA, Poelman EH, Tanaka T. 2013. Intrinsic inter- and intraspecific competition in parasitoid wasps. *Annu Rev Entomol* **58**:333–351. DOI: https://doi.org/10.1146/annurev-ento-120811-153622

Harvey JA, Strand MR. 2002. The developmental strategies of endoparasitoid wasps vary with host feeding ecology. *Ecology* **83**:2439–2451. DOI: https://doi.org/10.2307/3071805.

Heavner ME, Ramroop J, Gueguen G, Ramrattan G, Dolios G, Scarpati M, Kwiat J, Bhattacharya S, Wang R, Singh S, Govind S. 2017. Novel organelles with elements of bacterial and eukaryotic secretion systems weaponize parasites of *Drosophila*. *Curr Biol* **27**:2869-2877.e6. DOI: https://doi.org/10.1016/j.cub.2017.08.019

Holt C, Yandell M. 2011. MAKER2: an annotation pipeline and genome-database management tool for second-generation genome projects. *BMC Bioinformatics* **12**:491. DOI: https://doi.org/10.1186/1471-2105-12-491

Hotta M, Okuda T, Tanaka T. 2001. *Cotesia kariyai* teratocytes: growth and development. *Journal of Insect Physiology* **47**:31–41. DOI: https://doi.org/10.1016/S0022-1910(00)00089-5

Hu J, Fan J, Sun Z, Liu S. 2020. NextPolish: a fast and efficient genome polishing tool for long-read assembly. *Bioinformatics* **36**:2253–2255. DOI: https://doi.org/10.1093/bioinformatics/btz891

Huang J, Chen J, Fang G, Pang L, Zhou S, Zhou Y, Pan Z, Zhang Q, Sheng Y, Lu Y, Liu Z, Zhang Y, Li G, Shi M, Chen X, Zhan S. 2021. Two novel venom proteins underlie divergent parasitic strategies between a generalist and a specialist parasite. *Nat Commun* **12**:234. DOI: https://doi.org/10.1038/s41467-020-20332-8

Imai HT, Taylor RW, Crosland MW, Crozier RH. 1988. Modes of spontaneous chromosomal mutation and karyotype evolution in ants with reference to the minimum interaction hypothesis. *Jpn J Genet* **63**:159–185. DOI: https://doi.org/10.1266/jjg.63.159

Eggleton P, Belshaw R. 1992. Insect parasitoids: an evolutionary overview. *Phil Trans R Soc Lond B* **337**:1–20. DOI: https://doi.org/10.1098/rstb.1992.0079

Jia Q, Li S. 2023. Mmp-induced fat body cell dissociation promotes pupal development and moderately averts pupal diapause by activating lipid metabolism. *Proc Natl Acad Sci U S A* **120**:e2215214120. DOI: https://doi.org/10.1073/pnas.2215214120

Jia Q, Liu S, Wen D, Cheng Y, Bendena WG, Wang J, Li S. 2017. Juvenile hormone and 20-hydroxyecdysone coordinately control the developmental timing of matrix metalloproteinase-induced fat body cell dissociation. *J Biol Chem* **292**:21504–21516. DOI: https://doi.org/10.1074/jbc.M117.818880

Jones P, Binns D, Chang HY, Fraser M, Li W, McAnulla C, McWilliam H, Maslen J, Mitchell A, Nuka G, Pesseat S, Quinn AF, Sangrador-Vegas A, Scheremetjew M, Yong SY, Lopez R, Hunter S. 2014. InterProScan 5: genome-scale protein function classification. *Bioinformatics* **30**:1236–1240. DOI: https://doi.org/10.1093/bioinformatics/btu031

Kacsoh BZ, Lynch ZR, Mortimer NT, Schlenke TA. 2013. Fruit flies medicate offspring after seeing parasites. *Science* **339**:947–950. DOI: https://doi.org/10.1126/science.1229625

Katoh K, Misawa K, Kuma K, Miyata T. 2002. MAFFT: a novel method for rapid multiple sequence alignment based on fast Fourier transform. *Nucleic Acids Res* **30**:3059–3066. DOI: https://doi.org/10.1093/nar/gkf436

Kim D, Langmead B, Salzberg SL. 2015. HISAT: a fast spliced aligner with low memory requirements. *Nat Methods* **12**:357–360. DOI: https://doi.org/10.1038/nmeth.3317

Kim J, Chung YD, Park DY, Choi S, Shin DW, Soh H, Lee HW, Son W, Yim J, Park CS, Kernan MJ, Kim C. 2003. A TRPV family ion channel required for hearing in *Drosophila*. *Nature* **424**:81–84. DOI: https://doi.org/10.1038/nature01733

Knapp L, Mazzi D, Finger R. 2021. The economic impact of *Drosophila suzukii*: perceived costs and revenue losses of Swiss cherry, plum and grape growers. *Pest Manag Sci* **77**:978–1000. DOI: https://doi.org/10.1002/ps.6110.

Knoll V, Ellenbroek T, Romeis J, Collatz J. 2017. Seasonal and regional presence of hymenopteran parasitoids of *Drosophila* in Switzerland and their ability to parasitize the invasive *Drosophila suzukii*. *Sci Rep* **7**:40697. DOI: https://doi.org/10.1038/srep40697

Korf I. 2004. Gene finding in novel genomes. *BMC Bioinformatics* **5**:59. DOI:

https://doi.org/10.1186/1471-2105-5-59

Kremmer L, Thaon M, Borowiec N, David J, Poiri é M, Gatti JL, Ris N. 2017. Field monitoring of *Drosophila suzukii* and associated communities in south eastern France as a pre-requisite for classical biological control. *Insects* **8**:124. DOI: https://doi.org/10.3390/insects8040124

Lee JC, Wang X, Daane KM, Hoelmer KA, Isaacs R, Sial AA, Walton VM. 2019. Biological control of spotted-wing *Drosophila* (Diptera: Drosophilidae)—current and pending tactics. *Journal of Integrated Pest Management* **10**:13. DOI: https://doi.org/10.1093/jipm/pmz012

Letunic I, Bork P. 2021. Interactive Tree Of Life (iTOL) v5: an online tool for phylogenetic tree display and annotation. *Nucleic Acids Res* **49**:W293–W296. DOI: https://doi.org/10.1093/nar/gkab301

Li H. 2018. Minimap2: pairwise alignment for nucleotide sequences. *Bioinformatics* **34**:3094–3100. DOI: https://doi.org/10.1093/bioinformatics/bty191

Li H, Handsaker B, Wysoker A, Fennell T, Ruan J, Homer N, Marth G, Abecasis G, Durbin R, 1000 Genome Project Data Processing Subgroup. 2009. The sequence alignment/map format and SAMtools. *Bioinformatics* **25**:2078–2079. DOI: https://doi.org/10.1093/bioinformatics/btp352

Lieberman-Aiden E, van Berkum NL, Williams L, Imakaev M, Ragoczy T, Telling A, Amit I, Lajoie BR, Sabo PJ, Dorschner MO, Sandstrom R, Bernstein B, Bender MA, Groudine M, Gnirke A, Stamatoyannopoulos J, Mirny LA, Lander ES, Dekker J. 2009. Comprehensive mapping of long-range interactions reveals folding principles of the human genome. *Science* **326**:289–293. DOI: https://doi.org/10.1126/science.1181369

Liu TX, Stansly PA, Gerling D. 2015. Whitefly parasitoids: distribution, life history, bionomics, and utilization. *Annu Rev Entomol* **60**:273–292. DOI: https://doi.org/10.1146/annurev-ento-010814-021101

Martinson EO, Mrinalini, Kelkar YD, Chang CH, Werren JH. 2017. The Evolution of venom by co-option of single-copy genes. *Curr Biol* **27**:2007-2013.e8. DOI: https://doi.org/10.1016/j.cub.2017.05.032

Mazzetto F, Marchetti E, Amiresmaeili N, Sacco D, Francati S, Jucker C, Dindo ML, Lupi D, Tavella L. 2016. *Drosophila* parasitoids in northern Italy and their potential to attack the exotic pest *Drosophila suzukii*. *J Pest Sci* **89**:837–850. DOI: https://doi.org/10.1007/s10340-016-0746-7

Moran NA. 2002. Microbial minimalism: genome reduction in bacterial pathogens. *Cell* **108**:583–586. DOI: https://doi.org/10.1016/s0092-8674(02)00665-7

Moreau SJM, Asgari S. 2015. Venom proteins from parasitoid wasps and their biological functions. *Toxins (Basel)* **7**:2385–2412. DOI: https://doi.org/10.3390/toxins7072385

Mortimer NT, Goecks J, Kacsoh BZ, Mobley JA, Bowersock GJ, Taylor J, Schlenke TA. 2013. Parasitoid wasp venom SERCA regulates *Drosophila* calcium levels and inhibits cellular immunity. *Proc Natl Acad Sci U S A* **110**:9427–9432. DOI: https://doi.org/10.1073/pnas.1222351110

Muhlia-Almazán A, Sánchez-Paz A, García-Carreño FL. 2008. Invertebrate trypsins: a review. *J Comp Physiol B* **178**:655–672. DOI: https://doi.org/10.1007/s00360-008-0263-y

Müller CB, Schmid-Hempel P. 1993. Exploitation of cold temperature as defence against

parasitoids in bumblebees. *Nature* **363**:65–67. DOI: https://doi.org/10.1038/363065a0

Ode PJ, Vyas DK, Harvey JA. 2022. Extrinsic inter- and intraspecific competition in parasitoid wasps. *Annu Rev Entomol* **67**:305–328. DOI: https://doi.org/10.1146/annurev-ento-071421-073524

Pang L, Liu Z, Chen J, Dong Z, Zhou S, Zhang Q, Lu Y, Sheng Y, Chen X, Huang J. 2022. Search performance and octopamine neuronal signaling mediate parasitoid induced changes in Drosophila oviposition behavior. *Nat Commun* **13**:4476. DOI: https://doi.org/10.1038/s41467-022-32203-5

Patro R, Duggal G, Love MI, Irizarry RA, Kingsford C. 2017. Salmon provides fast and bias-aware quantification of transcript expression. *Nat Methods* **14**:417–419. DOI: https://doi.org/10.1038/nmeth.4197

Pedata PA, Garonna AP, Zabatta A, Zeppa P, Romani R, Isidoro N. 2003. Development and morphology of teratocytes in Encarsia berlesei and Encarsia citrina: first record for Chalcidoidea. *J Insect Physiol* **49**:1063–1071. DOI: https://doi.org/10.1016/j.jinsphys.2003.08.003

Pennacchio F, Strand MR. 2006. Evolution of developmental strategies in parasitic hymenoptera. *Annu Rev Entomol* **51**:233–258. DOI: https://doi.org/10.1146/annurev.ento.51.110104.151029

Perkins DN, Pappin DJC, Creasy DM, Cottrell JS. 1999. Probability-based protein identification by searching sequence databases using mass spectrometry data. *Electrophoresis* **20**:3551–3567. DOI: https://doi.org/10.1002/(SICI)1522-2683(19991201)20:18<3551::AID-ELPS3551>3.0.CO;2-2

Pertea M, Pertea GM, Antonescu CM, Chang TC, Mendell JT, Salzberg SL. 2015. StringTie enables improved reconstruction of a transcriptome from RNA-seq reads. *Nat Biotechnol* **33**:290–295. DOI: https://doi.org/10.1038/nbt.3122

Peters RS, Krogmann L, Mayer C, Donath A, Gunkel S, Meusemann K, Kozlov A, Podsiadlowski L, Petersen M, Lanfear R, Diez PA, Heraty J, Kjer KM, Klopfstein S, Meier R, Polidori C, Schmitt T, Liu S, Zhou X, Wappler T, Rust J, Misof B, Niehuis O. 2017. Evolutionary history of the hymenoptera. *Curr Biol* **27**:1013–1018. DOI: https://doi.org/10.1016/j.cub.2017.01.027 PMID: 28343967.

Polaszek A, Vilhemsen L. 2023. Biodiversity of hymenopteran parasitoids. *Current Opinion in Insect Science* **56**:101026. DOI: https://doi.org/10.1016/j.cois.2023.101026

Poirié M, Colinet D, Gatti JL. 2014. Insights into function and evolution of parasitoid wasp venoms. *Curr Opin Insect Sci* **6**:52–60. DOI: https://doi.org/10.1016/j.cois.2014.10.004

Poulin R, Randhawa HS. 2015. Evolution of parasitism along convergent lines: from ecology to genomics. *Parasitology* **142 Suppl 1**:S6–S15. DOI: https://doi.org/10.1017/S0031182013001674

Poyet M, Havard S, Prevost G, Chabrerie O, Doury G, Gibert P, Eslin P. 2013. Resistance of *Drosophila suzukii* to the larval parasitoids *Leptopilina heterotoma* and *Asobara japonica* is related to haemocyte load. *Physiological Entomology* **38**:45–53. DOI: https://doi.org/10.1111/phen.12002

Ramroop JR, Heavner ME, Razzak ZH, Govind S. 2021. A parasitoid wasp of *Drosophila* employs preemptive and reactive strategies to deplete its host's blood cells. *PLoS Pathog*

17:e1009615. DOI: https://doi.org/10.1371/journal.ppat.1009615

Rivers DB, Denlinger DL. 1995. Venom-induced alterations in fly lipid metabolism and its impact on larval development of the ectoparasitoid *Nasonia vitripennis* (Walker) (Hymenoptera: Pteromalidae). *Journal of Invertebrate Pathology* **66**:104–110. DOI: https://doi.org/10.1006/jipa.1995.1071

Rota-Stabelli O, Blaxter M, Anfora G. 2013. *Drosophila suzukii*. *Curr Biol* **23**:R8-9. DOI: https://doi.org/10.1016/j.cub.2012.11.021

Schütz S, Weissbecker B, Hummel HE, Apel KH, Schmitz H, Bleckmann H. 1999. Insect antenna as a smoke detector. *Nature* **398**:298–299. DOI: https://doi.org/10.1038/18585

Scott K, Brady R, Cravchik A, Morozov P, Rzhetsky A, Zuker C, Axel R. 2001. A chemosensory gene family encoding candidate gustatory and olfactory receptors in *Drosophila*. *Cell* **104**:661–673. DOI: https://doi.org/10.1016/s0092-8674(01)00263-x

Segoli M, Rosenheim JA. 2013. Limits to the reproductive success of two insect parasitoid species in the field. *Ecology* **94**:2498–2504. DOI: https://doi.org/10.1890/13-0262.1

Seppey M, Manni M, Zdobnov EM. 2019. BUSCO: Assessing genome assembly and annotation completeness. *Methods Mol Biol* **1962**:227–245. DOI: https://doi.org/10.1007/978-1-4939-9173-0_14

Shao E, Song Y, Wang Y, Liao Y, Luo Y, Liu S, Guan X, Huang Z. 2021. Transcriptomic and proteomic analysis of putative digestive proteases in the salivary gland and gut of *Empoasca* (*Matsumurasca*) *onukii* Matsuda. *BMC Genomics* **22**:271. DOI: https://doi.org/10.1186/s12864-021-07578-2

Smith SM. 1996. Biological control with *Trichogramma*: advances, successes, and potential of their use. *Annu Rev Entomol* **41**:375–406. DOI: https://doi.org/10.1146/annurev.en.41.010196.002111

Stamatakis A. 2014. RAxML version 8: a tool for phylogenetic analysis and post-analysis of large phylogenies. *Bioinformatics* **30**:1312–1313. DOI: https://doi.org/10.1093/bioinformatics/btu033

Stanke M, Diekhans M, Baertsch R, Haussler D. 2008. Using native and syntenically mapped cDNA alignments to improve de novo gene finding. *Bioinformatics* **24**:637–644. DOI: https://doi.org/10.1093/bioinformatics/btn013

Storer J, Hubley R, Rosen J, Wheeler TJ, Smit AF. 2021. The Dfam community resource of transposable element families, sequence models, and genome annotations. *Mob DNA* **12**:2. DOI: https://doi.org/10.1186/s13100-020-00230-y

Strand MR. 2014. Teratocytes and their functions in parasitoids. *Curr Opin Insect Sci* **6**:68–73. DOI: https://doi.org/10.1016/j.cois.2014.09.005

Suster ML, Seugnet L, Bate M, Sokolowski MB. 2004. Refining GAL4-driven transgene expression in *Drosophila* with a GAL80 enhancer-trap. *Genesis* **39**:240–245. DOI: https://doi.org/10.1002/gene.20051

van de Kamp T, Schwermann AH, Dos Santos Rolo T, Lösel PD, Engler T, Etter W, Faragó T, Göttlicher J, Heuveline V, Kopmann A, Mähler B, Mörs T, Odar J, Rust J, Tan Jerome N, Vogelgesang M, Baumbach T, Krogmann L. 2018. Parasitoid biology preserved in mineralized fossils. *Nat Commun* **9**:3325. DOI: https://doi.org/10.1038/s41467-018-05654-y

Vosshall LB, Amrein H, Morozov PS, Rzhetsky A, Axel R. 1999. A spatial map of olfactory receptor expression in the *Drosophila* antenna. *Cell* **96**:725–736. DOI: https://doi.org/10.1016/s0092-8674(00)80582-6

Vinson SB, Iwantsch GF. 1980. Host suitability for insect parasitoids. *Annu Rev Entomol* **25**: 397–419. DOI: https://doi.org/10.1146/annurev.en.25.010180.002145.

Wang XG, Serrato MA, Son Y, Walton VM, Hogg BN, Daane KM. 2018. Thermal performance of two indigenous pupal parasitoids attacking the invasive *Drosophila suzukii* (Diptera: Drosophilidae). *Environ Entomol* **47**:764–772. DOI: https://doi.org/10.1093/ee/nvy053

Wang ZZ, Ye XQ, Shi M, Li F, Wang ZH, Zhou YN, Gu QJ, Wu XT, Yin CL, Guo DH, Hu RM, Hu NN, Chen T, Zheng BY, Zou JN, Zhan LQ, Wei SJ, Wang YP, Huang JH, Fang XD, Strand MR, Chen XX. 2018. Parasitic insect-derived miRNAs modulate host development. *Nat Commun* **9**:2205. DOI: https://doi.org/10.1038/s41467-018-04504-1

Wang Z, Ren S, Zhan L, Wu Q, Huang J, Chen X. 2020. Species diversity of *Drosophila* and the associated parasitoid complex in waxberry orchard in Zhejiang Province. *Chinese Journal of Biological Control* **36**: 690–696.

Waterhouse RM, Seppey M, Simão FA, Manni M, Ioannidis P, Klioutchnikov G, Kriventseva EV, Zdobnov EM. 2018. BUSCO applications from quality assessments to gene prediction and phylogenomics. *Mol Biol Evol* **35**:543–548. DOI: https://doi.org/10.1093/molbev/msx319

Werren JH, Loehlin DW, Giebel JD. 2009. Larval RNAi in *Nasonia* (parasitoid wasp). *Cold Spring Harb Protoc* **2009**:pdb.prot5311. DOI: https://doi.org/10.1101/pdb.prot5311

Werren JH, Richards S, Desjardins CA, Niehuis O, Gadau J, Colbourne JK, The Nasonia Genome

Working Group, Beukeboom LW, Desplan C, Elsik CG, Grimmelikhuijzen CJP, Kitts P, Lynch JA, Murphy T, Oliveira DCSG, Smith CD, Zande L van de, Worley KC, Zdobnov EM, Aerts M, et al. 2010. Functional and evolutionary insights from the genomes of three parasitoid *Nasonia* species. *Science* **327**:343–348. DOI: https://doi.org/10.1126/science.1178028

Wertheim B. 2022. Adaptations and counter-adaptations in *Drosophila* host-parasitoid interactions: advances in the molecular mechanisms. *Curr Opin Insect Sci* **51**:100896. DOI: https://doi.org/10.1016/j.cois.2022.100896

Wicke S, Müller KF, de Pamphilis CW, Quandt D, Wickett NJ, Zhang Y, Renner SS, Schneeweiss GM. 2013. Mechanisms of functional and physical genome reduction in photosynthetic and nonphotosynthetic parasitic plants of the broomrape family. *Plant Cell* **25**:3711–3725. DOI: https://doi.org/10.1105/tpc.113.113373

Ye X, Yang Y, Zhao C, Xiao S, Sun YH, He C, Xiong S, Zhao X, Zhang B, Lin H, Shi J, Mei Y, Xu H, Fang Q, Wu F, Li D, Ye G. 2022. Genomic signatures associated with maintenance of genome stability and venom turnover in two parasitoid wasps. *Nat Commun* **13**:6417. DOI: https://doi.org/10.1038/s41467-022-34202-y

Yi C, Cai P, Lin J, Liu X, Ao G, Zhang Q, Xia H, Yang J, Ji Q. 2020. Life history and host preference of *Trichopria drosophilae* from southern China, one of the effective pupal parasitoids on the *Drosophila* species. *Insects* **11**:103. DOI: https://doi.org/10.3390/insects11020103

Yu H, Tian S, Huang Q, Chen J, Wu Y, Wang R, Lu L. 2021. An insect- and rain-proof net raises

the production and quality of Chinese bayberry by preventing damage from insects and altering bacterial communities. *Front Plant Sci* **12**:732012. DOI: https://doi.org/10.3389/fpls.2021.732012

Zhou S, Zhou Y, Wang Y, Chen J, Pang L, Pan Z, Li C, Shi M, Huang J, Chen X. 2019. The developmental transcriptome of *Trichopria drosophilae* (Hymenoptera: Diapriidae) and insights into cuticular protein genes. *Comp Biochem Physiol Part D Genomics Proteomics* **29**:245–254. DOI: https://doi.org/10.1016/j.cbd.2018.12.005

Figure legends

Figure 1. Chromosome-level assembly of a generalist drosophilid parasitoid genome.

(**A**) The life cycle of *T. drosophilae* (parasitoid) and *Drosophila* (host). *T. drosophila* (Td) is a pupal parasitoid that deposits eggs into *Drosophila* host pupae. As a generalist parasitoid, Td can successfully parasitize a variety of *Drosophila* species, including the well-known invasive pest *D. suzukii.* (**B**) and (**C**) The comparison of parasitization performance between Td and *A. japonica* (Aj). The parasitism rates (**B**) and wasp emergence rates (**C**) in six *Drosophila* species parasitized by Aj and Td. At least 5 biological replicates were performed. Data represent the mean ±SEM. Significance was analysed by two-way ANOVA with Sidak's multiple comparisons test (ns, not significant; $*p < 0.05$; $**p < 0.01$; $***p < 0.001$). *Dmel, D. melanogaster*; *Dsim, D. simulans*; *Dsan, D. santomea*; *Dere, D. erecta*; *Dsuz, D. suzukii*; *Dpse, D. pseudoobscura*; *Dvir, D. virilis.* (**D**) Genome size and repeat content of representative parasitoid species in the context of phylogeny. Parasitoid species were selected based on the presence of high-quality genome reference and the representativeness of the group. The corresponding host life-stage is shown in the coloured box. (**E**) The age and relative abundance of repeat element classes in Td genome. Kimura divergence from the consensus was estimated to indicate the burst time of repeats. See Figure 1—figure supplementary 2 for the plots of all involved parasitoid species.

Figure 2. Genomic distribution and expression profiling of *Timps* in Td.

(**A**) Top 20 expanded functional domains in Td genome in comparison to other parasitoids. Species abbreviations correspond to those in Figure 1D. (**B**) Genomic locations of characterized *Timp* genes on Td chromosomes. (**C**) Maximum-likelihood phylogenetic tree across all identified Timp in insects. The copies in Td are highlighted in color. The colors also correspond to those on (**B**) and (**D**). (**D**) Transcriptome expression profiles of *Timp* genes across different developmental stages and representative tissues. The phylogeny is based on the expression pattern.

Figure 3. Td venom glands recruit a family of Timp as venom proteins to arrest the host development.

(**A**) Schematic diagram of Td parasitization and venom injection into *Drosophila* host pupa. Wasp venom is produced in the venom gland (VG) and stored in the venom reservoir (VR). (**B**) and (**C**) Development of *D. suzukii* (**B**) and *D. melanogaster* (**C**) pupae treated by Td parasitization and venom injections. One-day-old host pupae were either parasitized by Td or injected with wasp venom at 1: 20 and 1: 40 dilutions or PBS (CK). Fly eyes are marked by red arrowheads, and bristles are marked by yellow arrowheads. Here, darker red eye colour and bristle appearance represent the older development of host pupae. Scale bar: 400 μm. More than 40 host pupae were examined for each group. (**D**) Identification and annotation of venom proteins (VPs). The expression value in the VGs and its specialization level are presented on the x-axis and y-axis, respectively. The specialized index was estimated by the ratio of expression in VGs to the mean value of any other tissues and developmental stages (Supplementary Table S3). (**E**) Schematic

illustration of the temperature-sensitive conditional GAL4/GAL80^{ts} system to drive *UAS-Timp* expression in host pupae. At the permissive temperature (18 ℃), binding of GAL80^{ts} to GAL4 prevented the transcription of *Timp* genes. After shifting to 29 ℃, GAL80^{ts} was inactivated, allowing *da-GAL4* to ubiquitously activate the transcription of *Timp* genes. (**F**) Development of *D. melanogaster* pupae after ectopic expression of *D. melanogaster Timp* (*DmTimp*) and *TdTimps.* One-day-old *D. melanogaster* pupae were transferred from 18 ℃ to 29 ℃ using the GAL4/GAL80^{ts} system to ubiquitously overexpress *Timp* genes in host pupae. Fly eyes are marked by red arrowheads, and bristles are marked by yellow arrowheads. Here, darker red eye colour and bristle appearance represent the older development of host pupae. The outline around each representative image refers to the pupa case. Scale bar: 400 μm. More than 40 host pupae were examined for each group.

Figure 4. Td teratocytes secret trypsin proteins to digest host tissues.

(**A**) Schematic diagram of teratocytes in Td-parasitized *Drosophila* hosts. Teratocytes are derived from the serosal membrane during Td egg hatching. (**B**) Transmission electron microscopy of Td teratocytes. Details of the micrograph (red box) showing the perinuclear region containing abundant rough endoplasmic reticulum (RER), numerous mitochondria (M), Golgi apparatus (G), and vesicles (V). Note that microvilli (MV) are obvious on the external surface of the teratocyte membrane, and the nucleus (N) is relatively large. Scale bars: shown in the images. (**C**) *D. suzukii* host tissues, including the brain, testis and ovary, were cocultured with teratocytes derived from a single parasitized host. Host tissues cocultured with Schneider's medium only were used as

controls (CK). The status of the host tissues was recorded after 0 h, 12 h and 30 h of incubation. Scale bars: 200 μm. More than 20 tissues were examined for each group. (**D**) Identification of effecting components in teratocytes. The expression value in the teratocytes and associated specialized level to other tissues and developmental stages are presented on the x-axis and y-axis, respectively. The specialized index was calculated as the ratio of expression value in teratocytes to the mean value of other tissues and developmental stages (Supplementary Table S4). (**E**) Different concentrations of a trypsin inhibitor, TLCK, were added to the mixtures of *D. suzukii* testes and teratocytes. The status of the host tissues was recorded after 0 h and 30 h of incubation. Scale bars: 200 μm. More than 20 testes were examined for each group. (**F**) The wasp emergence rate in *D. suzukii* parasitized by Td after injection of different amounts of TLCK (20 ng, 200 ng, 400 ng per host pupa). ddH_2O injection was used as a control (CK). Three biological replicates were performed. Data represent the mean ± SEM. Significance was analysed by one-way ANOVA with Sidak's multiple comparisons test. Different letters indicate statistically significant differences ($p < 0.05$). **(G)** Representative images of Td larvae in CK and TLCK-injected hosts after 96 h and 144 h parasitization. Scale bars: 200 μm. More than 20 larvae were examined for each group.

Figure 5. Superparasitism enhances Td parasitic efficiency.

(**A**) and (**B**) Parasitism rates (**A**) and wasp emergence rates (**B**) in 1- to 4-day-old *D. suzukii* pupae after monoparasitism or superparasitism by Td. Six biological replicates were performed. Data represent the mean ± SEM. Significance was analysed by two-way ANOVA with Sidak's multiple comparisons test (ns, not significant; $^{**}p < 0.01$; $^{***}p < 0.001$). (**C**) The images and body length

of Td males and females emerged from young and old *D. suzukii* hosts. n = 38 and 35 male wasps, n = 39 and 34 female wasps, respectively. Data represent the mean ± SEM. Significance was determined by two-tailed unpaired Student's t tests (***$p < 0.001$). Scale bar: 500 μm. (**D**) The size of the venom gland (VG) and venom reservoir (VR) of Td females emerged from young and old *D. suzukii* hosts. Left to right: n = 33, 31, 33 and 31 wasps. Data represent the mean ± SEM. Significance was determined by two-tailed unpaired Student's t tests (***$p < 0.001$). Scale bar: 100 μm. (**E**) The ovaries and egg load of Td females emerged from young and old *D. suzukii* hosts. n = 33 and 30 wasps, respectively. Data represent the mean ± SEM. Significance was determined by two-tailed unpaired Student's t tests (***$p < 0.001$). Scale bar: 400 μm. (**F**) Schematic diagram of the Td oviposition choice assays. One-day-old host pupae were placed on the left side, and the same number of X-day-old host pupae (X = 1, 2, 3, or 4) were placed on the right side. Oviposition index = $(N_1 - N_x)/(N_1 + N_x) \times 100\%$, where N_1 is the total number of wasp eggs in the host pupae on the left and N_x is the total number of wasp eggs in the host pupae on the right. (**G**) Oviposition indices of Td females in different aged *D. suzukii* hosts from 2 h and 4 h assays. Five biological replicates were performed. Box plots represent the median (bold black line), quartiles (boxes), and minimum and maximum (whiskers). All oviposition indices were not significantly different from zero (bold red line), which represents no choice for Td egg laying. Deviation of the oviposition index against zero was tested with the Wilcoxon signed rank test (ns, not significant). Young host: 1-day-old pupae; old host: 4-day-old pupae.

Figure 6. Td avoids interspecific competition through chemoreception in the ovipositor. (**A**) Schematic diagram of the Td interspecific competition assay. PH, Aj-parasitized host; NH, non-parasitized host. (**B**) Oviposition rates of Td in NH and PH pupae of *D. suzukii* and *D. melanogaster*, respectively. At least five biological replicates were performed. Data represent the mean ± SEM. Significance was analysed by the Mann-Whitney U test ($^{**}p < 0.01$). (**C**) Schematic diagram Td ovipositor, which contains two ovipositor sheaths and one ovipositor stylet. (**D**) to (**I**) Transmission electron microscope micrograph of Td ovipositor stylet. Higher magnification micrographs show the proximal end (**E**, Region I in **D**) and distal end (**F**, II in **D**) of the ovipositor stylet. Different types of sensilla (arrowheads) on ventral (v) and dorsal (d) valves are identified, including secretary pores (SP, red arrowhead) (**G**), surface-dome sensilla (SD, green arrowhead) (**H**) and coeloconic sensilla (CS, yellow arrowhead) (**I**). Scale bars are shown in the images. (**J**) Principal component analysis based on overall expression profiles across different tissues. (**K**) Expression profiles of Td genes in ovipositors and female antennae. Each dot indicates the log-transformed expression values (TPM) in ovipositors (x-axis) and in female antennae (y-axis).

Figure 7. Genomic distribution and expression profiling of gustatory receptor genes in Td. (**A**) Genomic location of characterized gustatory receptor (GR) genes on Td chromosomes. (**B**) Transcriptome expression profiles of GR genes across representative tissues. The phylogeny is based on the expression pattern. (**C**) qPCR verification of selective GRs with high expression in ovipositors.

Figure 8. Proposed model of the molecular and ecological adaptions underlying the parasitic success in Td.

Td is a solitary parasitoid that presents high levels of pupal parasitism to *Drosophila* species, including *D. suzukii*. Td allows intraspecific superparatism to increase the success of wasp emergence from hosts with the help of two weapons. Specifically, two Timp VPs trigger the development arrest of *Drosophila* hosts, eventually leading to the maintenance of the hosts at a younger status, whereas trypsins in teratocytes contribute to the digestion of host tissues, providing suitable nutritional resources for the wasp larvae. Moreover, Td avoids interspecific competition with larval parasitoid species to extend their parasitic efficacy and mostly depends on chemoreception on the ovipositor.

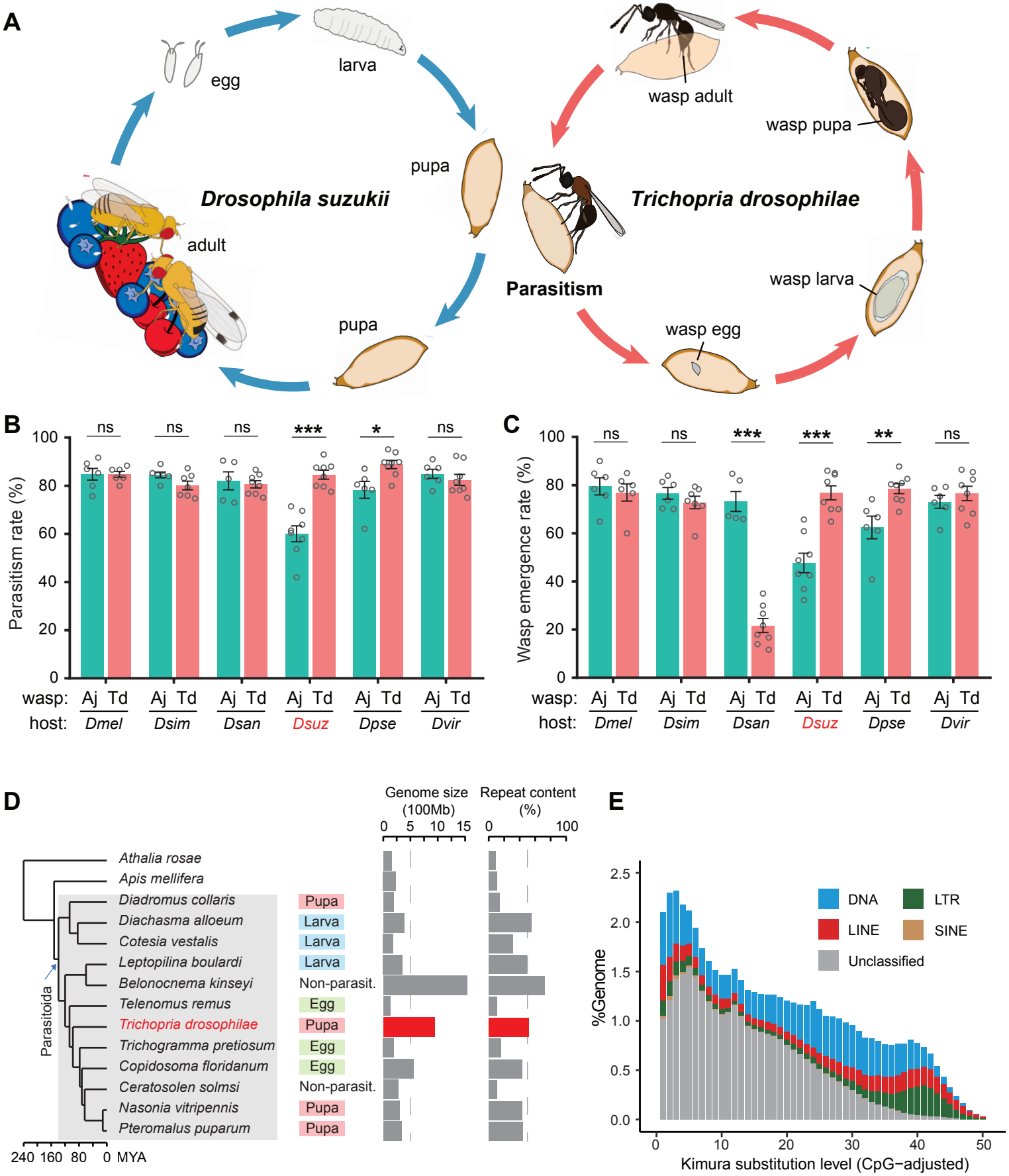
A
egg
larva
pupa
adult
pupa
Drosophila suzukii
wasp adult
wasp pupa
Trichopria drosophilae
Parasitism
wasp larva
wasp egg
B
Parasitism rate (%)
ns
ns
ns
***
*
ns
wasp: Aj Td Aj Td Aj Td Aj Td Aj Td Aj Td
host: Dmel Dsim Dsan Dsuz Dpse Dvir
C
Wasp emergence rate (%)
ns
ns
***
***
**
ns
wasp: Aj Td Aj Td Aj Td Aj Td Aj Td Aj Td
host: Dmel Dsim Dsan Dsuz Dpse Dvir
D
Genome size (100Mb)
Repeat content (%)
Athalia rosae
Apis mellifera
Diadromus collaris
Diachasma alloeum
Cotesia vestalis
Leptopilina boulardi
Belonocnema kinseyi
Telenomus remus
Trichopria drosophilae
Trichogramma pretiosum
Copidosoma floridanum
Ceratosolen solmsi
Nasonia vitripennis
Pteromalus puparum
Pupa
Larva
Larva
Larva
Non-parasit.
Egg
Pupa
Egg
Egg
Non-parasit.
Pupa
Pupa
Parasitoida
240 160 80 0 MYA
E
%Genome
DNA
LTR
LINE
SINE
Unclassified
Kimura substitution level (CpG−adjusted)

Figure 1

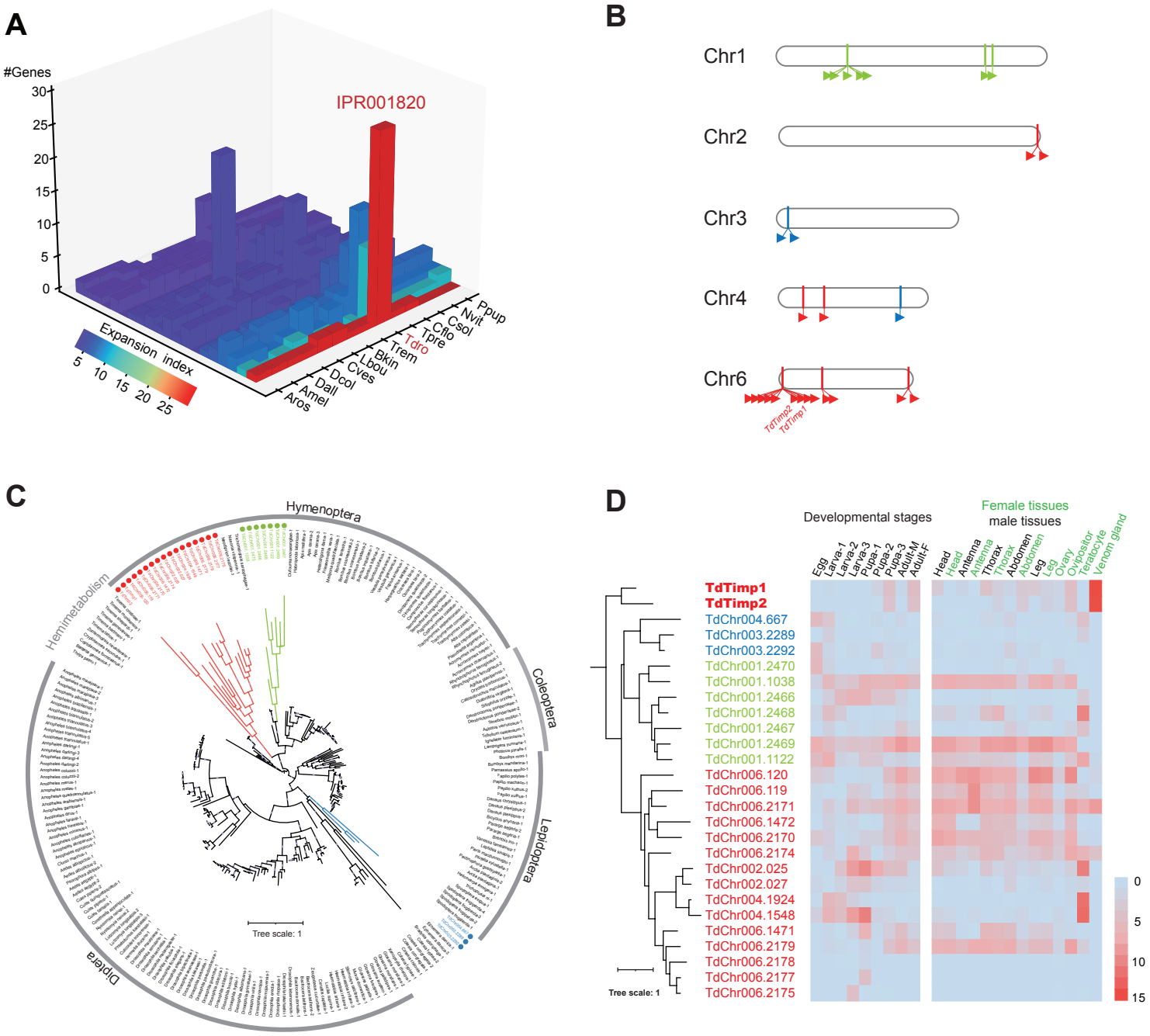
A
#Genes
30
25
20
15
10
5
0
IPR001820
Expansion index
5 10 15 20 25
Aros
Amel
Dall
Dcol
Cves
Lbou
Bkin
Trem
Tdro
Tpre
Cflo
Csol
Nvit
Ppup
B
Chr1
Chr2
Chr3
Chr4
Chr6
TdTimp2
TdTimp1
C
Hymenoptera
Hemimetabolism
Coleoptera
Lepidoptera
Diptera
Tree scale: 1
D
Developmental stages
Female tissues
male tissues
Egg
Larva-1
Larva-2
Larva-3
Pupa-1
Pupa-2
Pupa-3
Adult-M
Adult-F
Head
Head
Antenna
Antenna
Thorax
Abdomen
Leg
Leg
Ovary
Ovipositor
Teratocyte
Venom gland
TdTimp1
TdTimp2
TdChr004.667
TdChr003.2289
TdChr003.2292
TdChr001.2470
TdChr001.1038
TdChr001.2466
TdChr001.2468
TdChr001.2467
TdChr001.2469
TdChr001.1122
TdChr006.120
TdChr006.119
TdChr006.2171
TdChr006.1472
TdChr006.2170
TdChr006.2174
TdChr002.025
TdChr002.027
TdChr004.1924
TdChr004.1548
TdChr006.1471
TdChr006.2179
TdChr006.2178
TdChr006.2177
TdChr006.2175
Tree scale: 1
0
5
10
15

Figure 2

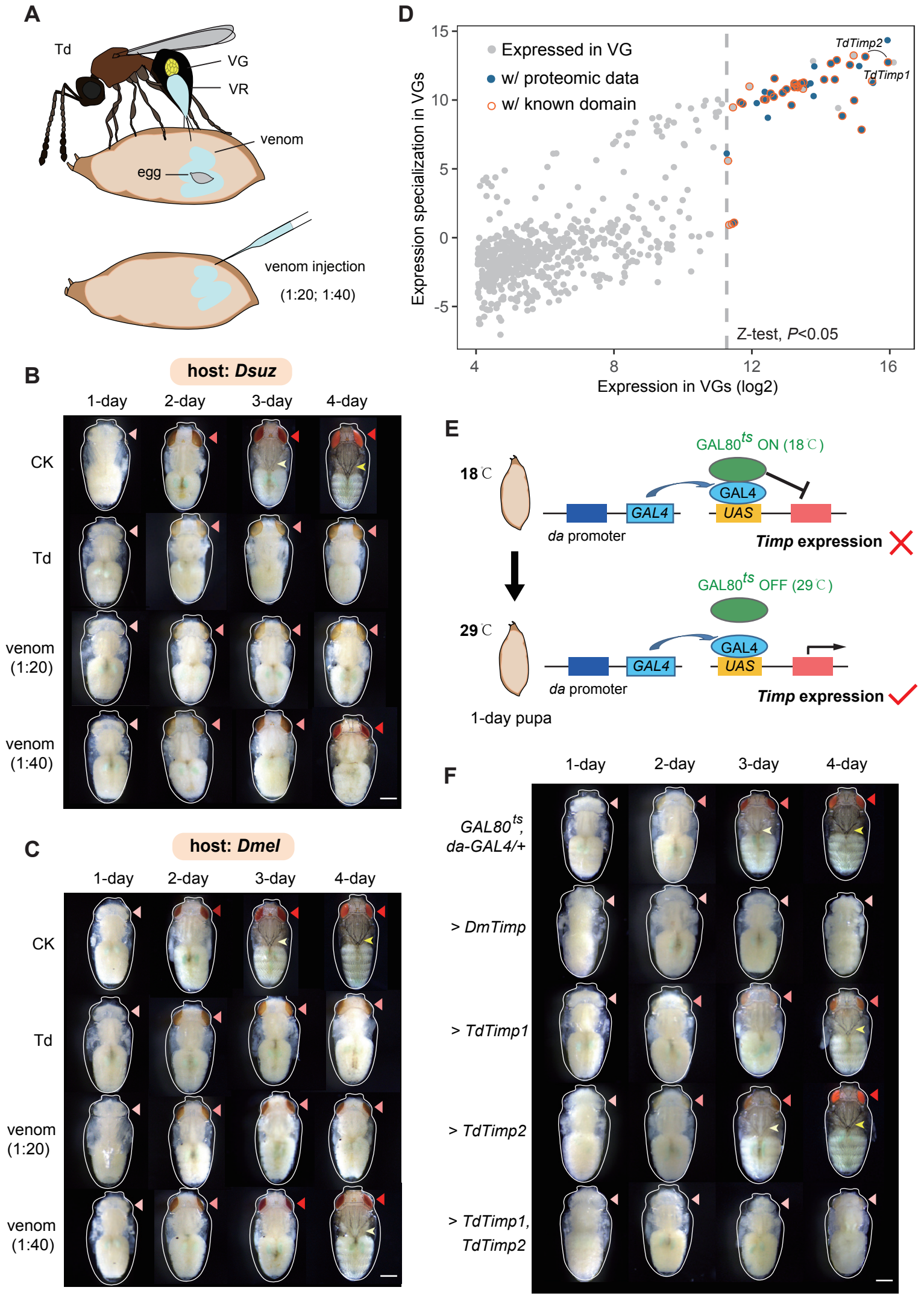
A
Td
VG
VR
venom
egg
venom injection
(1:20; 1:40)
D
Expressed in VG
w/ proteomic data
w/ known domain
TdTimp2
TdTimp1
Z-test, P<0.05
Expression specialization in VGs
Expression in VGs (log2)
B
host: Dsuz
1-day
2-day
3-day
4-day
CK
Td
venom (1:20)
venom (1:40)
E
18℃
GAL80ts ON (18℃)
GAL4
UAS
da promoter
Timp expression
29℃
GAL80ts OFF (29℃)
1-day pupa
C
host: Dmel
F
GAL80ts, da-GAL4/+
> DmTimp
> TdTimp1
> TdTimp2
> TdTimp1, TdTimp2

Figure 3

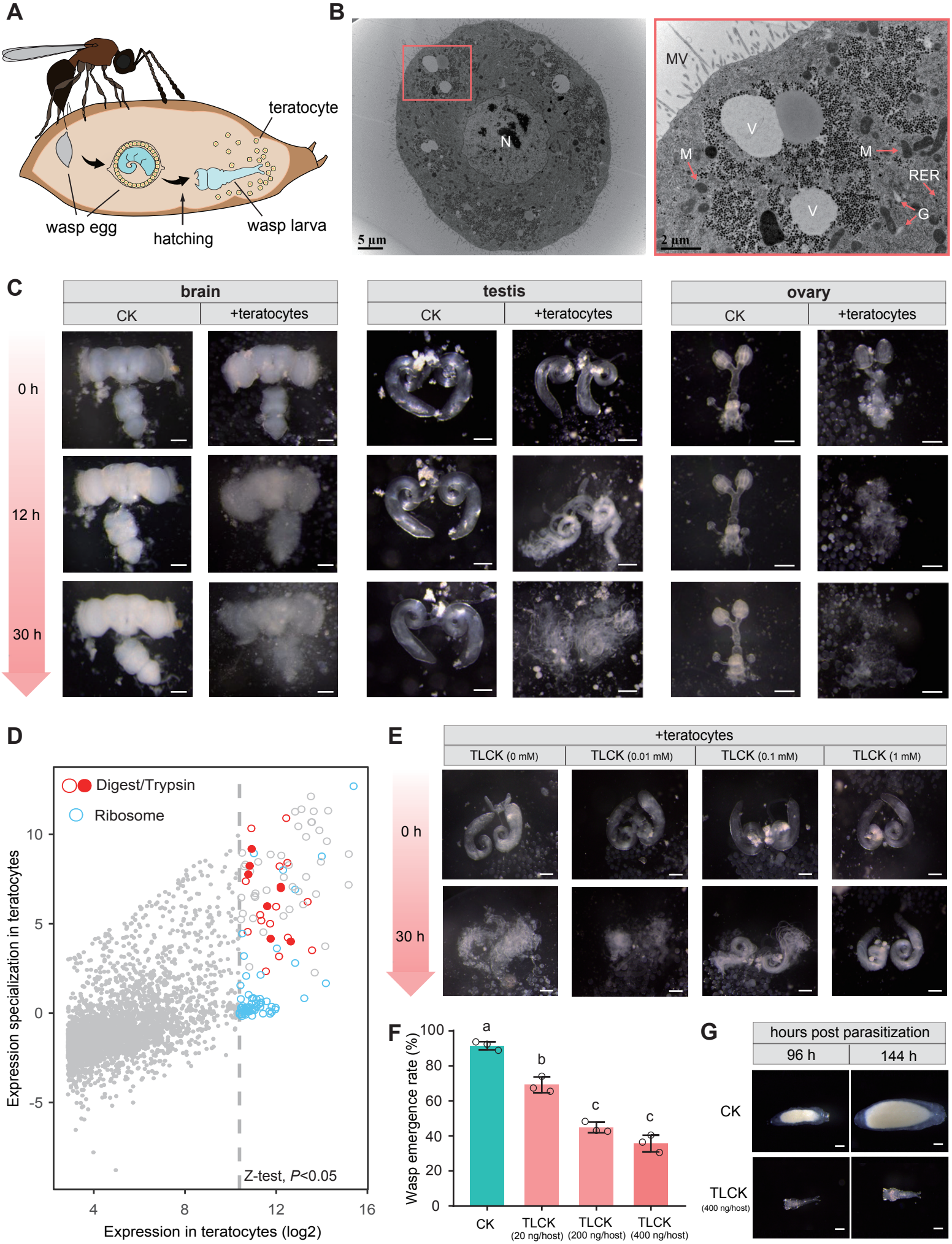
A
teratocyte
wasp egg
hatching
wasp larva
B
N
5 μm
MV
V
M
M
RER
V
G
2 μm
C
brain
CK
+teratocytes
testis
CK
+teratocytes
ovary
CK
+teratocytes
0 h
12 h
30 h
D
Digest/Trypsin
Ribosome
Expression specialization in teratocytes
Expression in teratocytes (log2)
Z-test, P<0.05
E
+teratocytes
TLCK (0 mM)
TLCK (0.01 mM)
TLCK (0.1 mM)
TLCK (1 mM)
0 h
30 h
F
Wasp emergence rate (%)
a
b
c
c
CK
TLCK (20 ng/host)
TLCK (200 ng/host)
TLCK (400 ng/host)
G
hours post parasitization
96 h
144 h
CK
TLCK (400 ng/host)

Figure 4

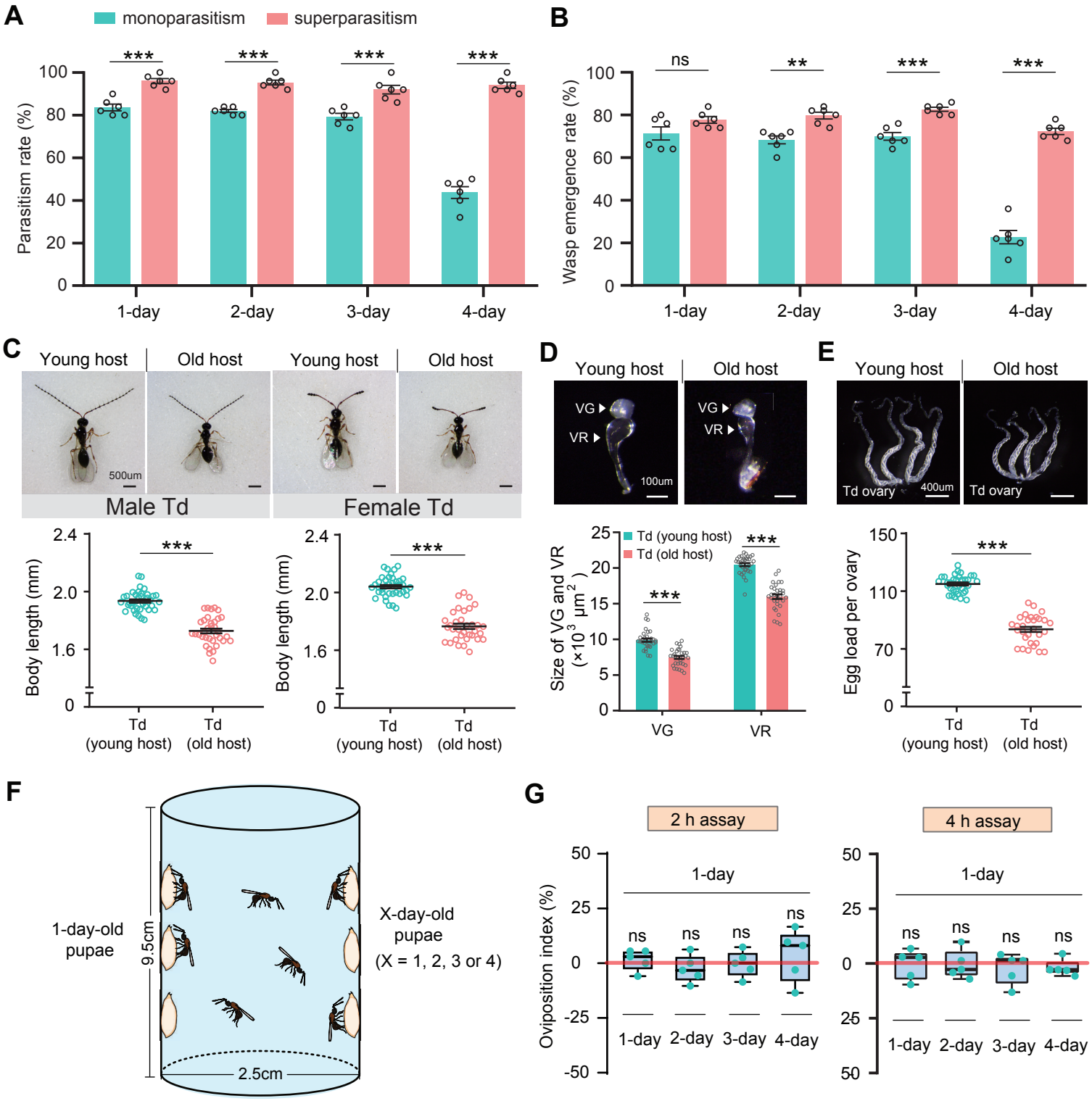
A
monoparasitism
superparasitism
Parasitism rate (%)
1-day
2-day
3-day
4-day
B
Wasp emergence rate (%)
ns
C
Young host
Old host
500um
Male Td
Female Td
Body length (mm)
Td (young host)
Td (old host)
D
VG
VR
100um
Size of VG and VR (×10³ μm²)
E
Td ovary
400um
Egg load per ovary
F
1-day-old pupae
9.5cm
2.5cm
X-day-old pupae (X = 1, 2, 3 or 4)
G
2 h assay
4 h assay
Oviposition index (%)

Figure 5

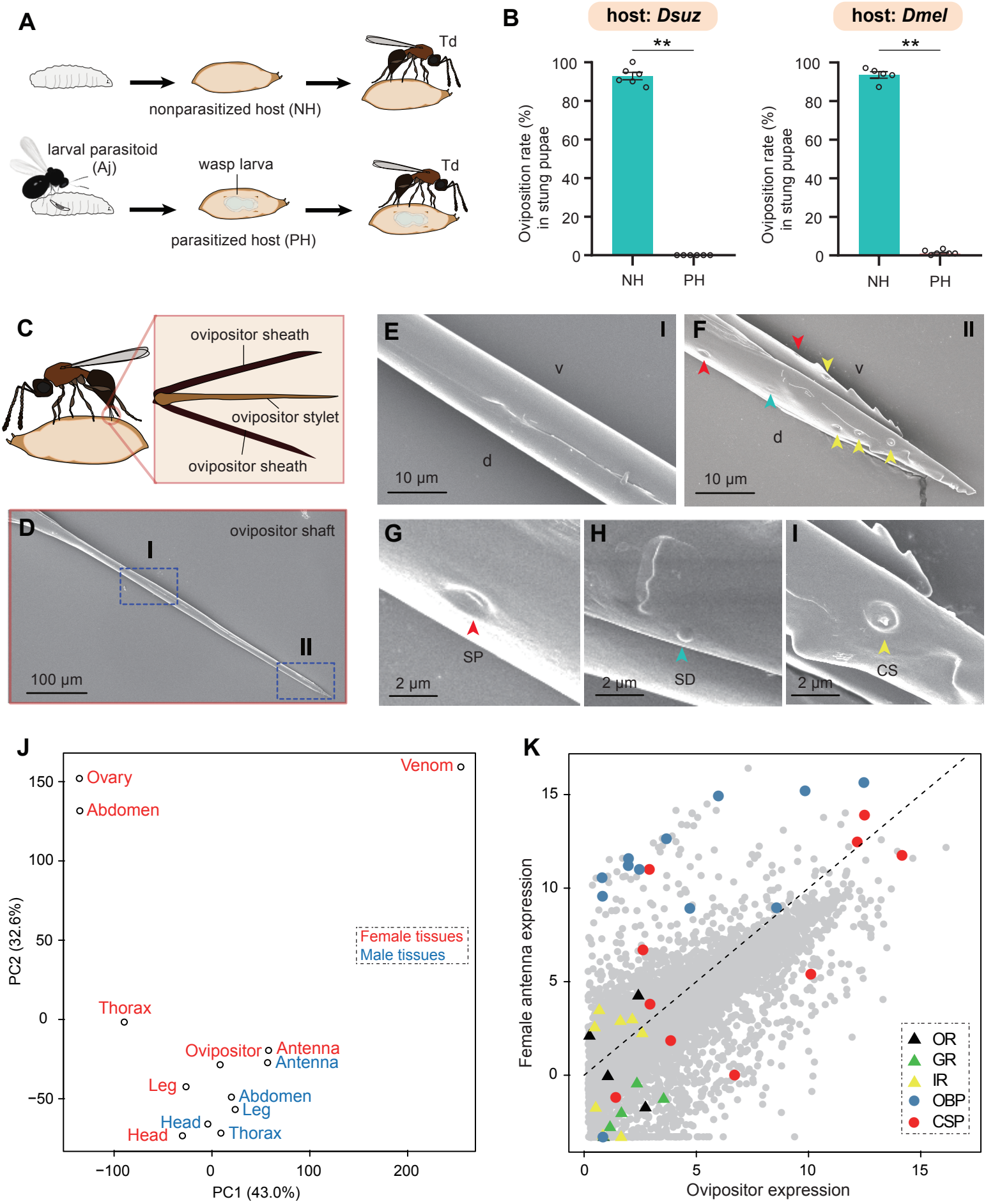
A
Td
nonparasitized host (NH)
larval parasitoid
(Aj)
wasp larva
Td
parasitized host (PH)
B
host: Dsuz
host: Dmel
**
**
Oviposition rate (%)
in stung pupae
100
80
60
40
20
0
NH
PH
C
ovipositor sheath
ovipositor stylet
ovipositor sheath
D
ovipositor shaft
I
II
100 μm
E
I
v
d
10 μm
F
II
v
d
10 μm
G
SP
2 μm
H
SD
2 μm
I
CS
2 μm
J
Venom
Ovary
Abdomen
Female tissues
Male tissues
Thorax
Ovipositor
Antenna
Antenna
Leg
Abdomen
Leg
Head
Head
Thorax
PC2 (32.6%)
PC1 (43.0%)
150
100
50
0
−50
−100
0
100
200
K
Female antenna expression
Ovipositor expression
15
10
5
0
OR
GR
IR
OBP
CSP

Figure 6

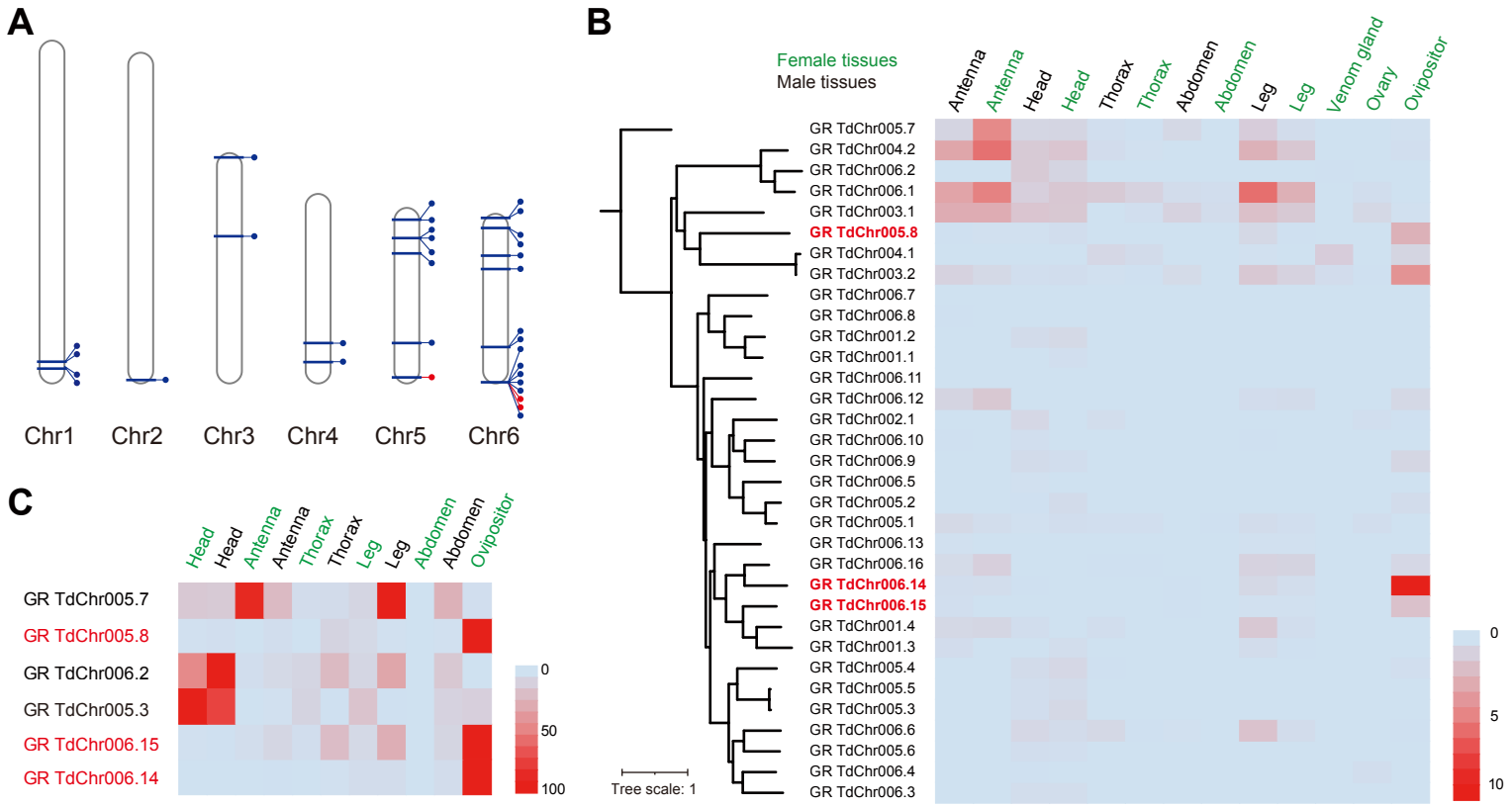
A
Chr1
Chr2
Chr3
Chr4
Chr5
Chr6
B
Female tissues
Male tissues
Antenna
Antenna
Head
Head
Thorax
Thorax
Abdomen
Abdomen
Leg
Leg
Venom gland
Ovary
Ovipositor
GR TdChr005.7
GR TdChr004.2
GR TdChr006.2
GR TdChr006.1
GR TdChr003.1
GR TdChr005.8
GR TdChr004.1
GR TdChr003.2
GR TdChr006.7
GR TdChr006.8
GR TdChr001.2
GR TdChr001.1
GR TdChr006.11
GR TdChr006.12
GR TdChr002.1
GR TdChr006.10
GR TdChr006.9
GR TdChr006.5
GR TdChr005.2
GR TdChr005.1
GR TdChr006.13
GR TdChr006.16
GR TdChr006.14
GR TdChr006.15
GR TdChr001.4
GR TdChr001.3
GR TdChr005.4
GR TdChr005.5
GR TdChr005.3
GR TdChr006.6
GR TdChr005.6
GR TdChr006.4
GR TdChr006.3
Tree scale: 1
0
5
10
C
Head
Head
Antenna
Antenna
Thorax
Thorax
Leg
Leg
Abdomen
Abdomen
Ovipositor
GR TdChr005.7
GR TdChr005.8
GR TdChr006.2
GR TdChr005.3
GR TdChr006.15
GR TdChr006.14
0
50
100

Figure 7

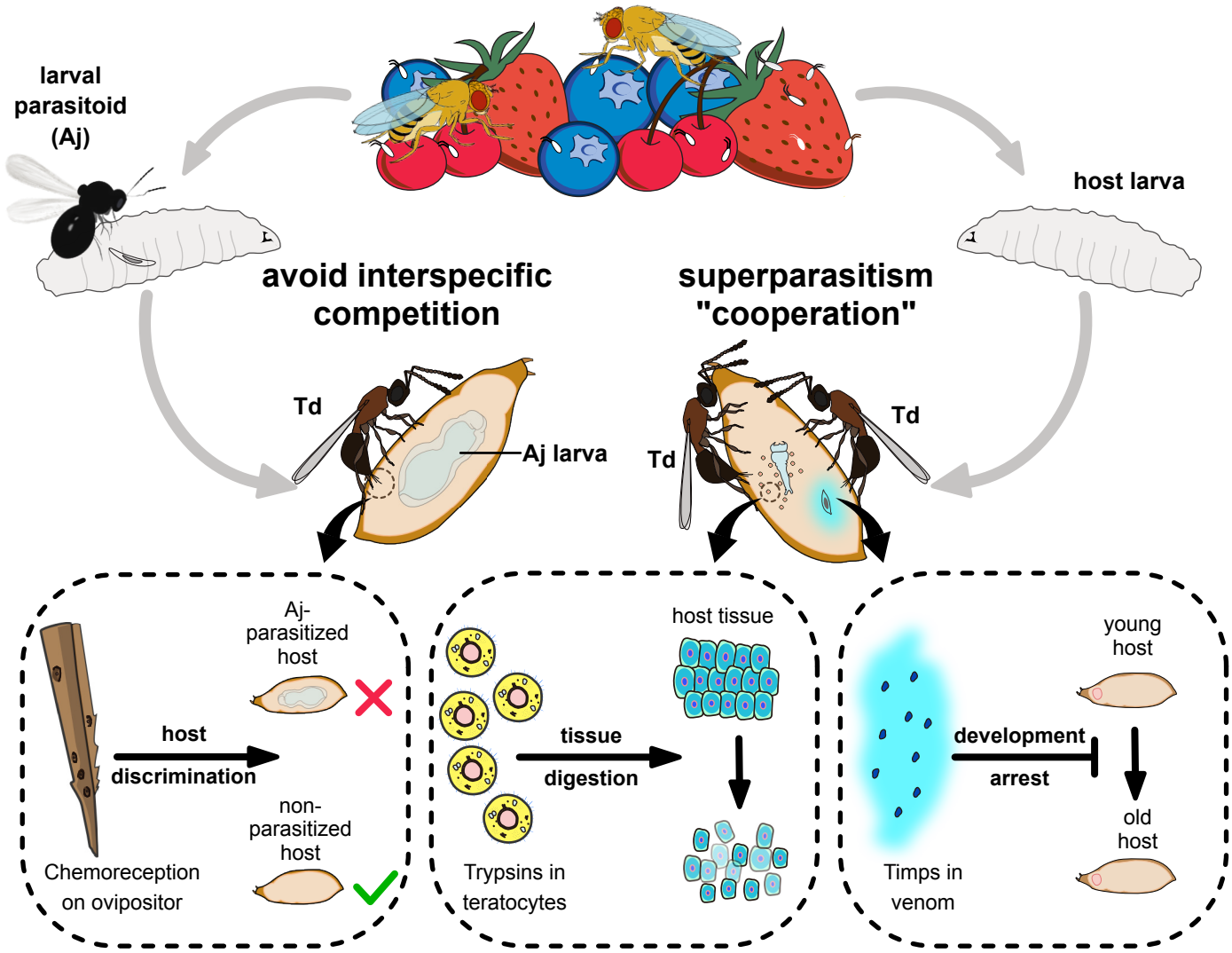
larval
parasitoid
(Aj)
host larva
avoid interspecific
competition
superparasitism
"cooperation"
Td
Aj larva
Td
Td
Aj-
parasitized
host
host
discrimination
non-
parasitized
host
Chemoreception
on ovipositor
host tissue
tissue
digestion
Trypsins in
teratocytes
young
host
development
arrest
old
host
Timps in
venom

Figure 8

Supplementary Information for

Coordinated molecular and ecological adaptations underlie a highly successful parasitoid

Supplementary information includes supplementary figures and supplementary tables.

Supplementary Tables S1-S8 are presented in a separated Excel file.

Table S1 Basic features of *Trichopria drosophilae* genome

Table S2 Top 20 expanded gene families in Td

Table S3 List of Td venom protein genes

Table S4 List of Td teratocyte genes

Table S5 List of Td chemoreception genes

Table S6 Primer sequences in this study

Table S7 Transcriptome sequencing data in this study

Table S8 Raw data in Figure 1—figure supplement 1D

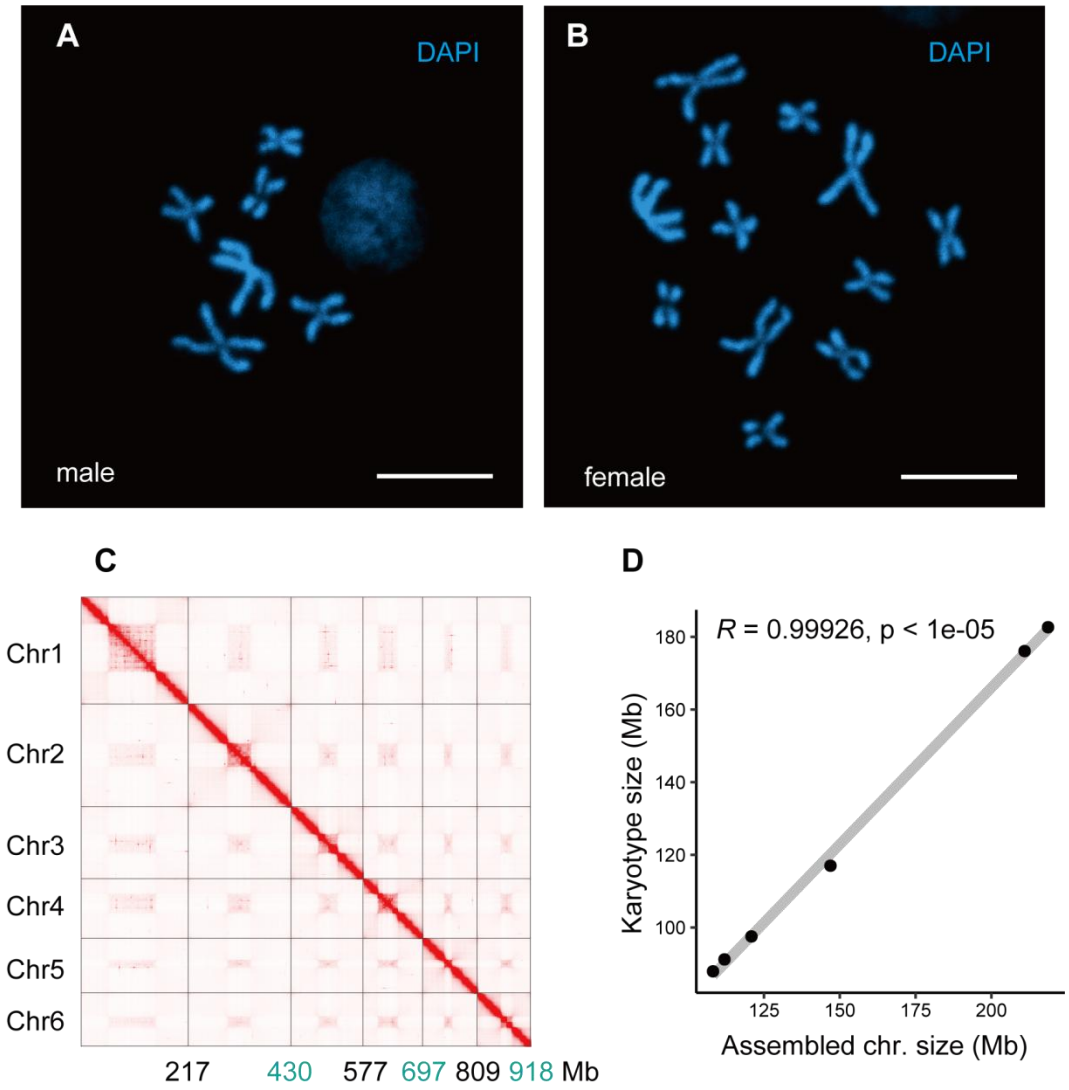

Figure 1—figure supplement 1. Chromosome features of Td.

(**A**) Chromosome staining of male Td haploid chromosome (n = 6). Scale bars: 10 µm. (**B**) Chromosome staining of female Td diploid chromosome sets (2n = 12). Scale bars: 10 µm. (**C**) The heatmap of Hi-C all-by-all interaction among 6 chromosomes of Td. The y axis refers each chromosome. The x axis refers every chromosome with assembly scaffold length. The frequency of Hi-C interaction links is represented by the color, which ranges from white (low) to red (high). The map indicates that intrachromosomeinteractions (red blocks in the diagonal) were stronger than interchromosome interactions (white blocks). (**D**) Correlation between estimated chromosome sizes (in Mb) based on karyotype images and assembled scaffolds. The values on Y-axis indicate the estimated karyotype size of a chromosome, which is calculated based on collected the chromosome size and the length of chromosome in karyotype images of closely related species (*Aphelinus varipes*). Then we used them as a reference to obtain the estimated karyotype chromosome sizes basing on the length of chromosomes in the karyotype images of Td. Each dot indicates a single chromosome. The correlation coefficient is 0.99926, indicating near good correlation between chromosomal scaffold length and karyotypically determined chromosome length. Raw data was provided in Supplementary file Table S8.

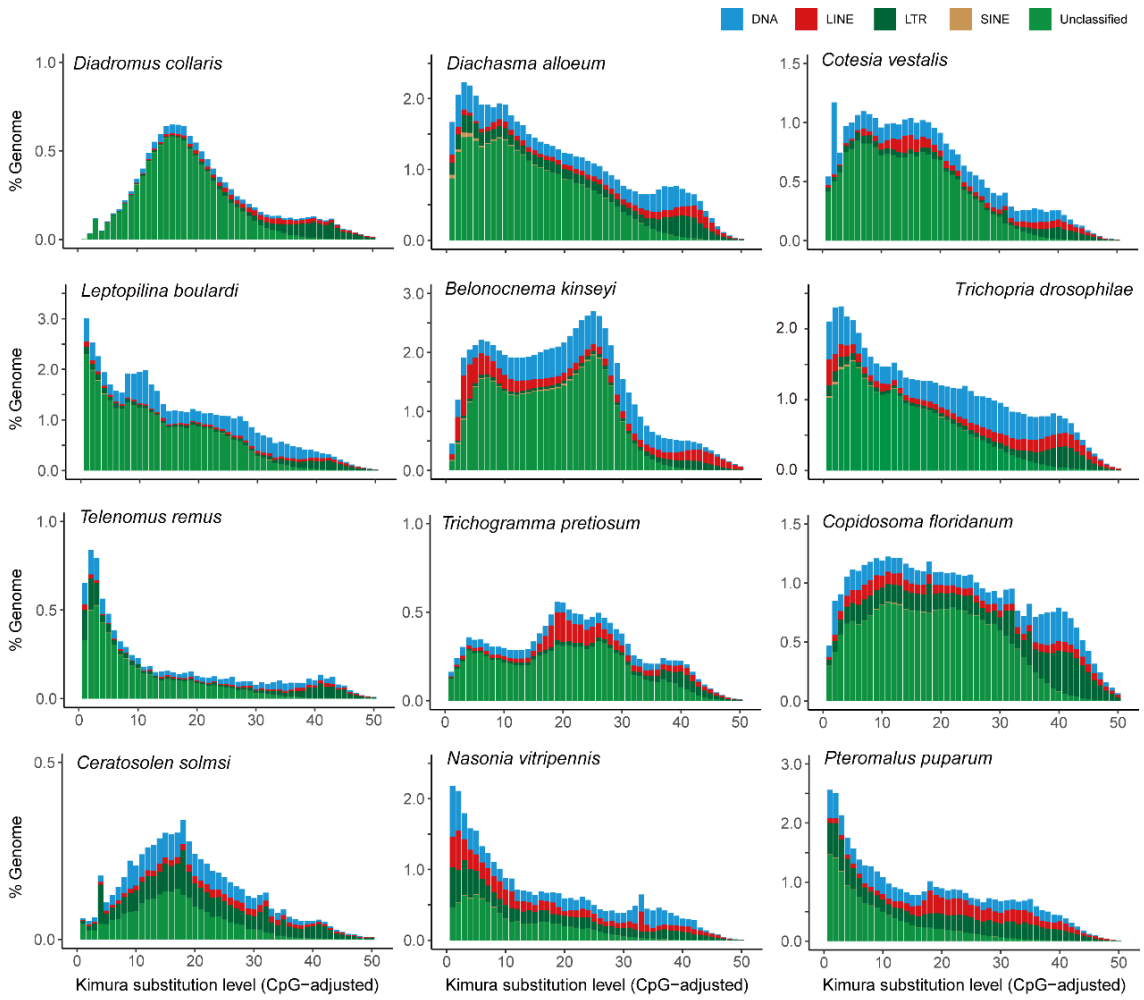

Figure 1—figure supplement 2. Distribution of repeat content among representative parasitoid species.

The age and relative abundance of repeat element classes across representative parasitoid genomes. The CpG-adjusted Kimura divergence from the consensus was estimated to indicate the time of duplication.

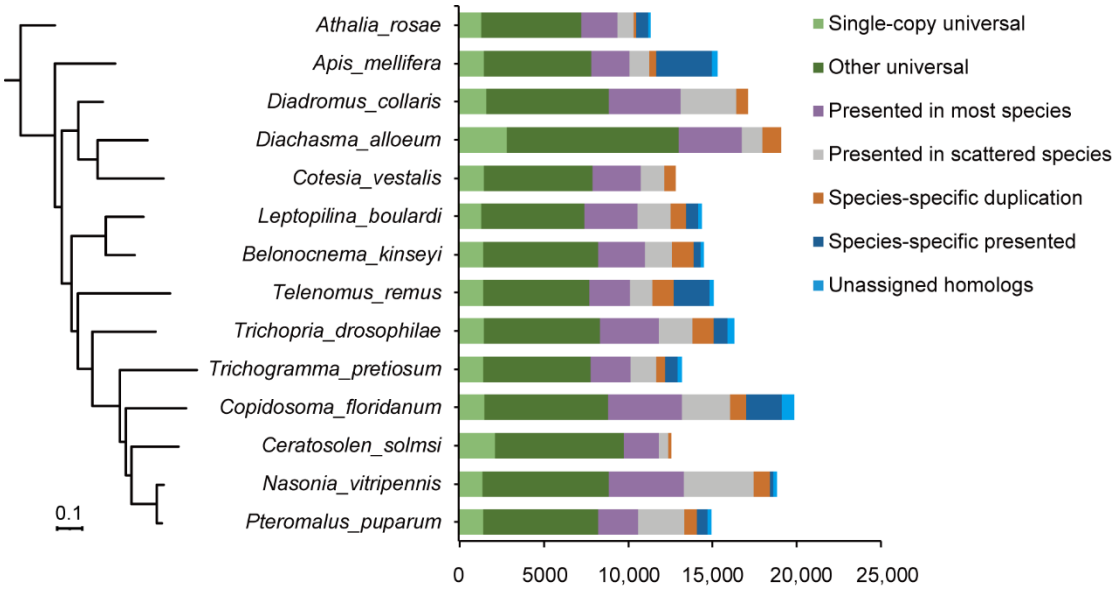

Figure 1—figure supplement 3. Phylogeny and ortholog content across representative parasitoid species.

The phylogeny on the left is a maximum-likelihood phylogenetic tree based 1246 single-copy orthologs across 12 representative species with high-quality reference genomes as well we two related hymenopteran species. The assignment of ortholog contents is shown as histograms on the right.

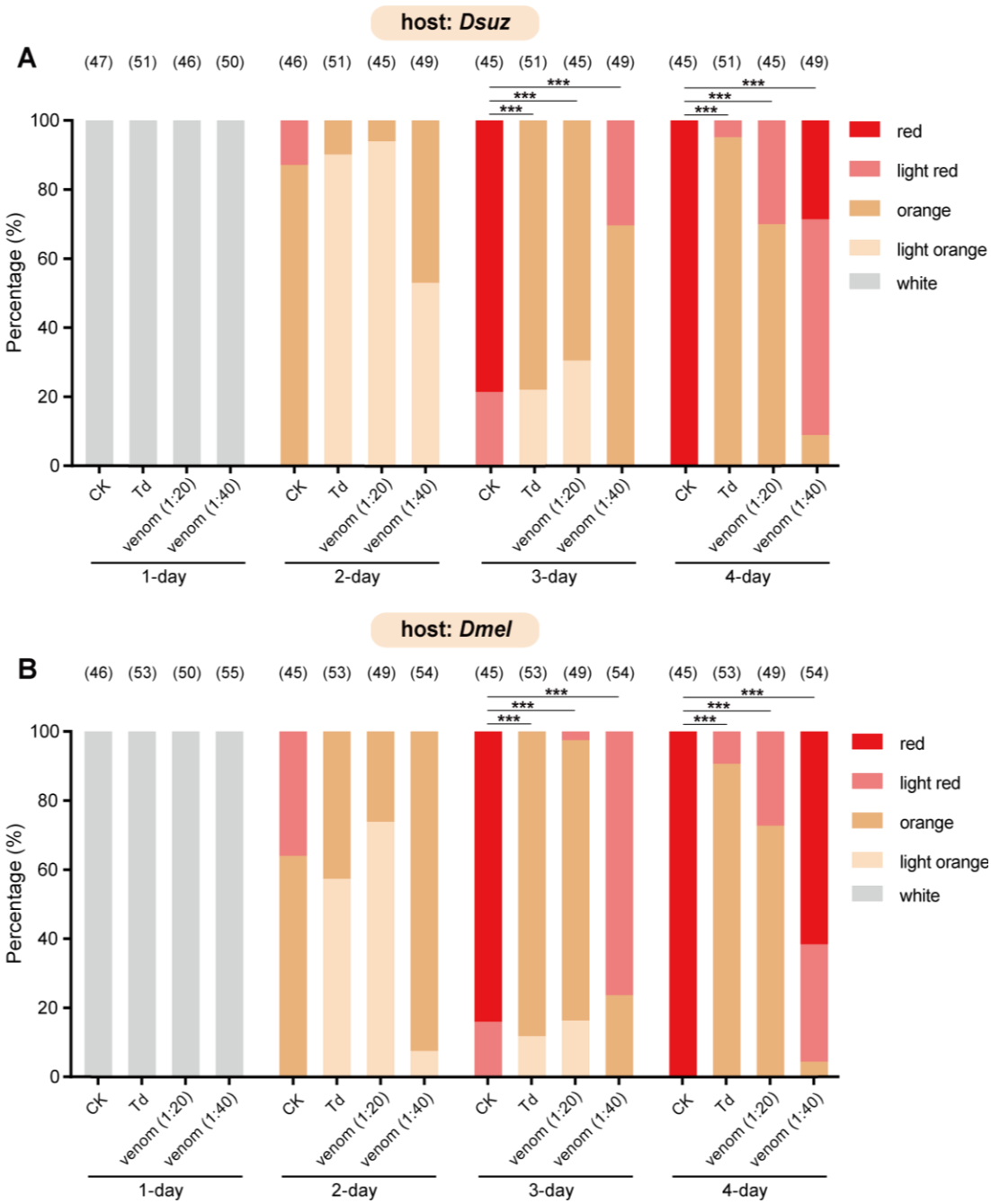

Figure 3—figure supplement 1. Characterization of the developmental delay phenotype in Figure 3B (A) and Figure 3C (B).

The eye colors of *Drosophila* hosts were divided into 5 levels from white (young) to red (old), including white, light orange, orange, light red, and red. The percentage of *D. suzukii* (**A**) and *D. melanogaster* (**B**) pupae with different eye colors were quantified. Significance of the proportion of red eye pupae was analyzed by Fisher's exact test (***$p < 0.001$). The n value of each experiment was provided above the column.

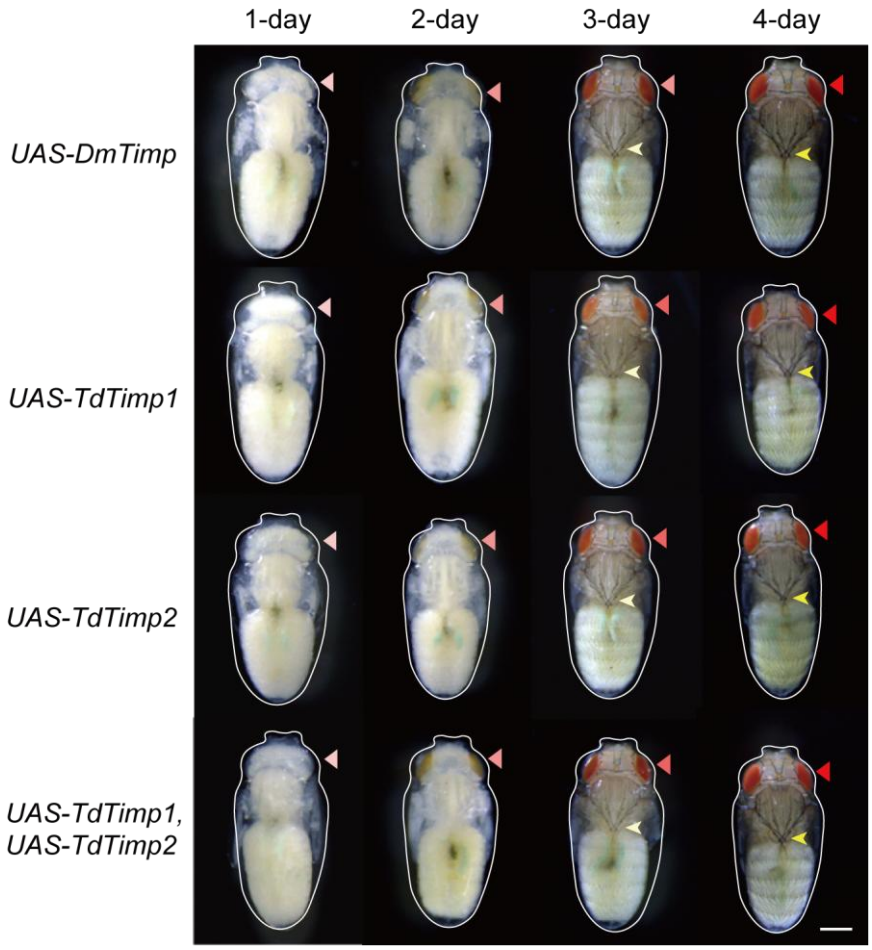

Figure 3—figure supplement 2. Development of *D. melanogaster* UAS-controls.
The UAS-controls for Figure 3F, including UAS-DmTimp, UAS-TdTimp1, UAS-TdTimp2, and UAS-TdTimp1+ TdTimp2. Fly eyes are marked by red arrowheads, and bristles are marked by yellow arrowheads. The outline around each animal refers to the pupa case. Scale bar: 400 μm.

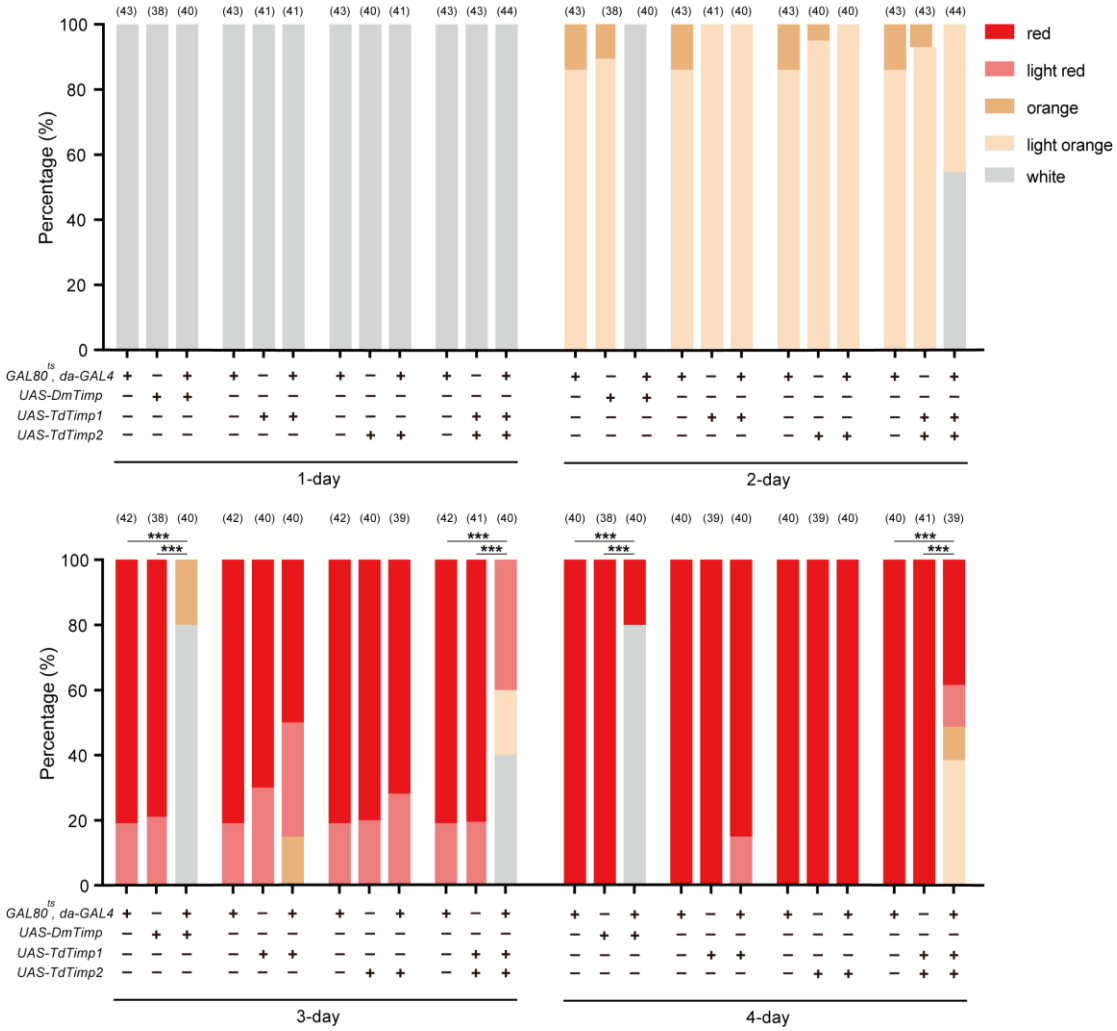

Figure 3—figure supplement 3. Characterization of the developmental delay phenotype in Figure 3F and Figure 3—figure supplement 2.

The eye colors of *D. melanogaster* were divided into 5 levels from white (young) to red (old), including white, light orange, orange, light red, and red. The percentage of *D. melanogaster* pupae with different eye colors were quantified. Significance of the proportion of red eye pupae was analyzed by Fisher's exact test (***$p < 0.001$). The n value of each experiment was provided above the column.

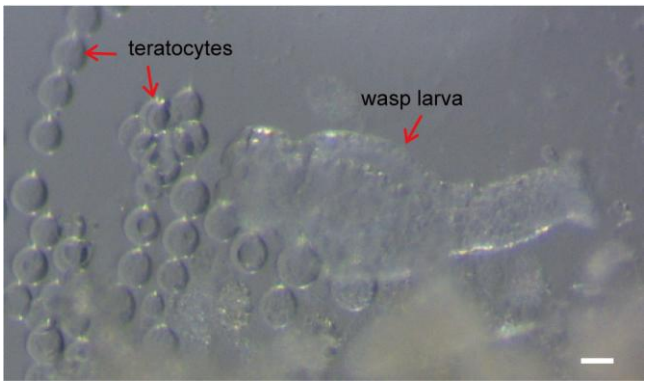

Figure 4—figure supplement 1. The teratocytes are released during Td egg hatching. A Td egg was dissected and cultured in Schneider's medium (Thermo Fisher Scientific, Cat#21720001). When the egg hatched into a larva in the culture medium, it released teratocytes as well. Scale bar: 100 μm.

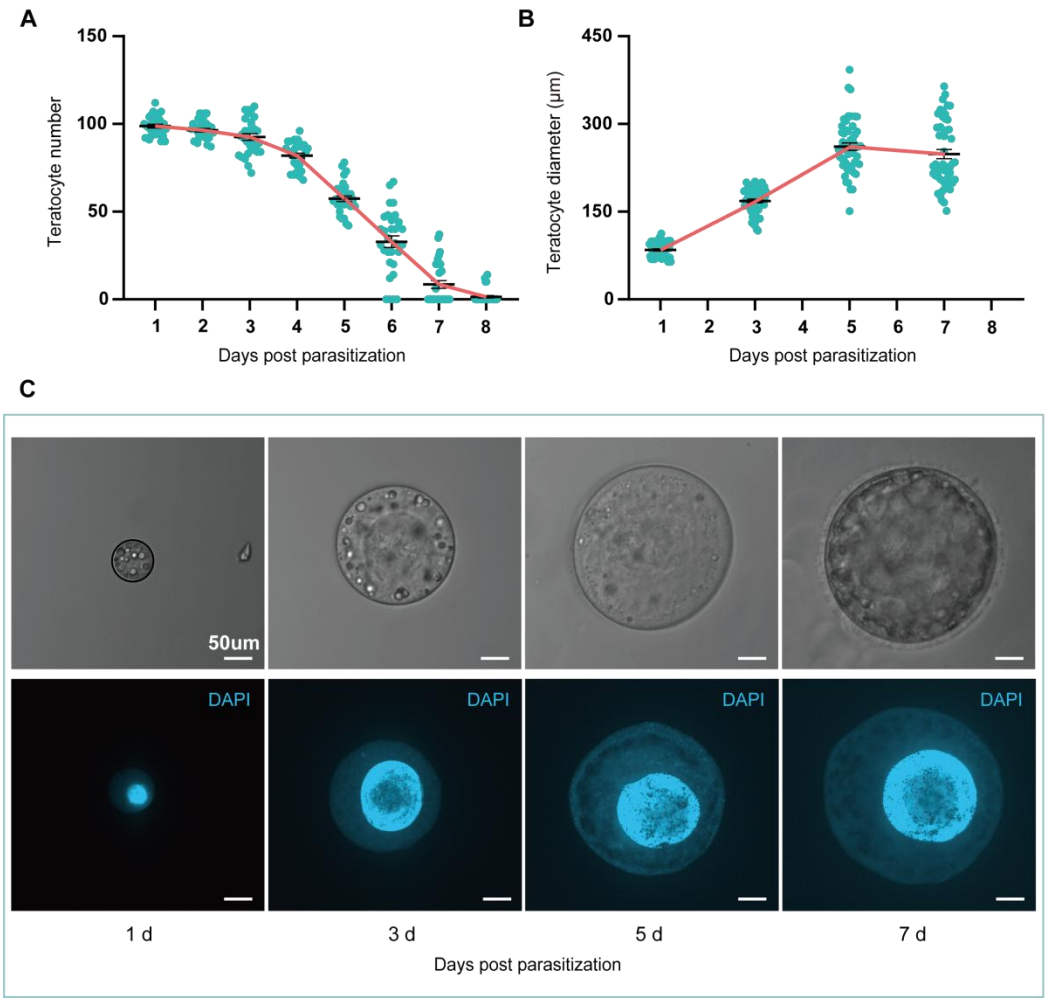

Figure 4—figure supplement 2. The size and number of teratocytes in parasitized hosts. (**A**) The teratocyte numbers in single *D. suzukii* host of different days post Td parasitization. n = 31 for each group. (**B**) The teratocyte diameters in *D. suzukii* host of different days post Td parasitization. Left to right, n = 52, 53, 52 and 50 teratocytes. (**C**) The Light microscopy images and DAPI staining images of teratocytes in *D. suzukii* host of different days post Td parasitization. Scale bars: 50 μm. At least 20 teratocytes were examined for each group.

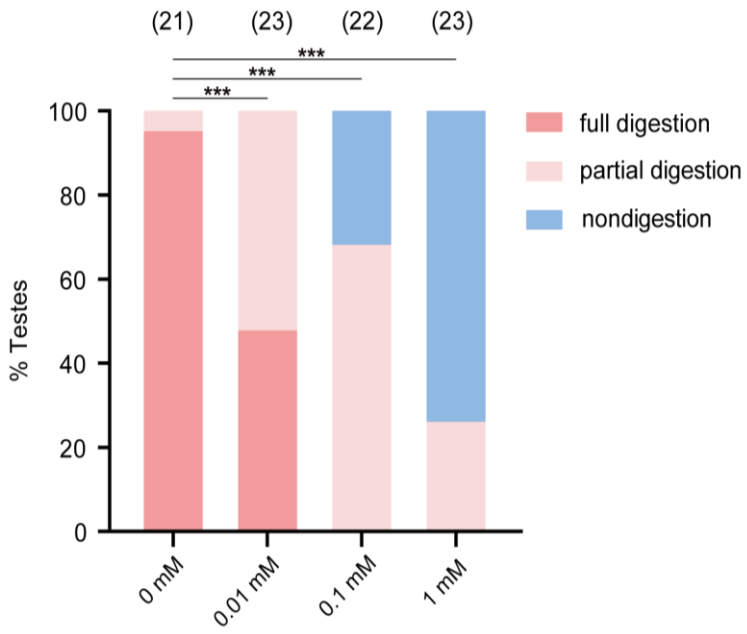

Figure 4—figure supplement 3. A trypsin inhibitor, TPCK, impairs the degradation function of teratocyte.

The percentage of host tissue at different digestion status in Figure 4E after incubation with a trypsin inhibitor, TLCK. Significance of the proportion of full digestion was analyzed by Fisher's exact test (***$p < 0.001$). The n value of each experiment was provided above the column.

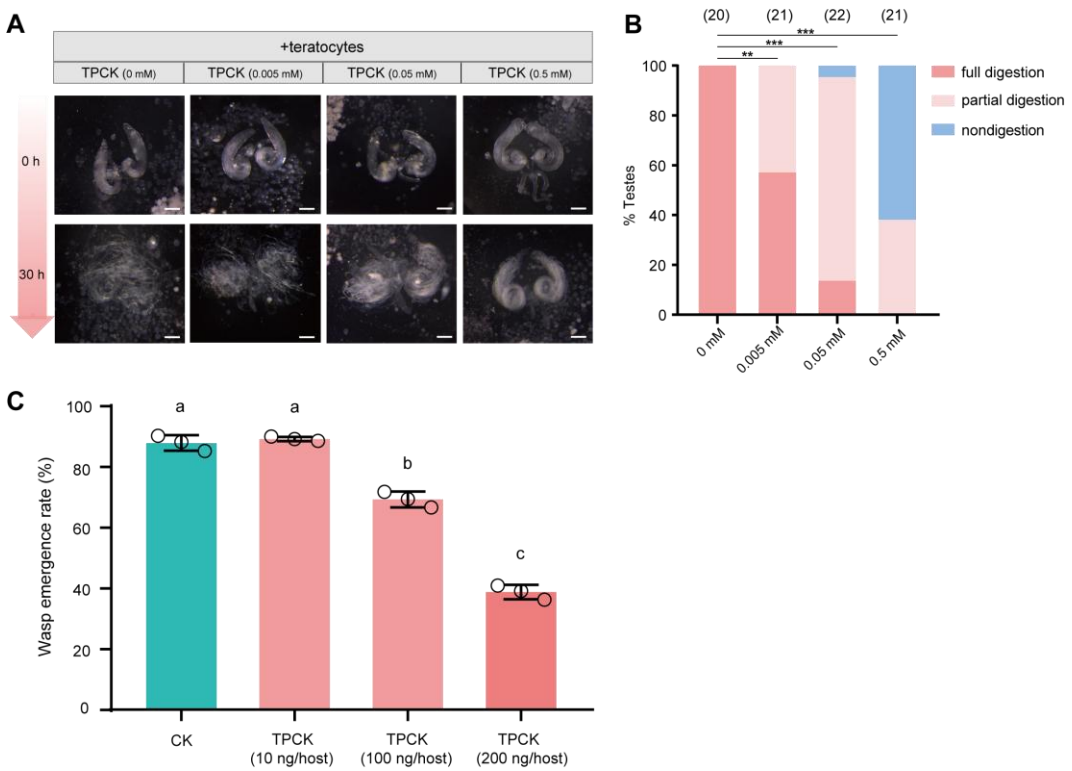

Figure 4—figure supplement 4. A trypsin inhibitor, TPCK, impairs the degradation function of teratocyte.

(**A**) Different concentrations of a trypsin inhibitor, TPCK, were added to the mixtures of *D. suzukii* testes and teratocytes. The status of the host tissues were recorded after 0 h, and 30 h incubation. Scale bars: 200 µm. At least 20 testes were examined for each group. (**B**) The percentage of host tissue at different digestion status in (**A**). Significance of the proportion of full digestion was analyzed by Fisher's exact test (**$p < 0.01$, ***$p < 0.001$). The n value of each experiment was provided above the column. (**C**) The wasp emergence rate in *D. suzukii* parasitized by Td after injection different amounts of TPCK (10 ng, 100 ng, 200 ng per host pupa). DMSO injection was used as a control (CK). Three biological replicates were performed. Data represent the mean ± SEM. Significance was analyzed by one-way ANOVA with Sidak's multiple comparisons test. Different letters indicate statistically significant differences ($p < 0.05$).

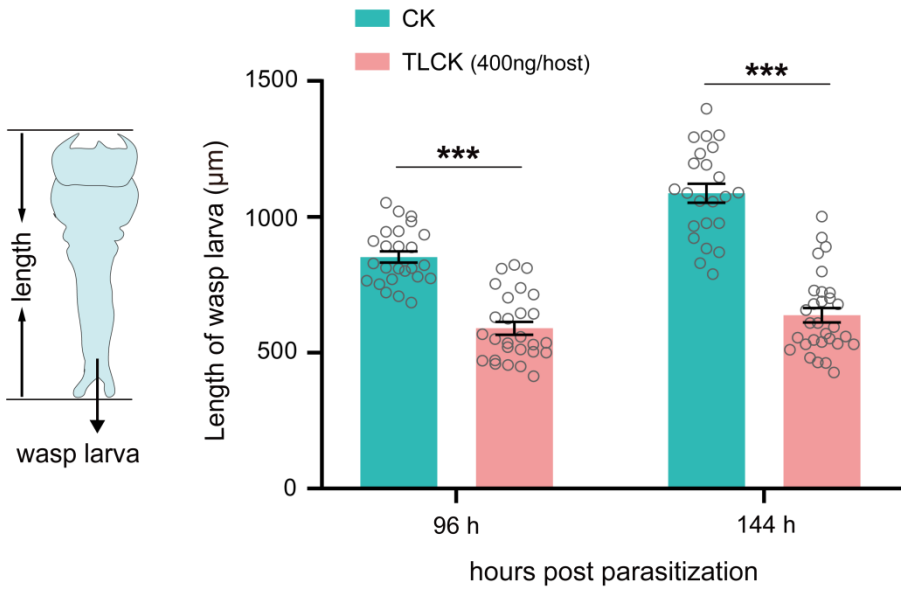

Figure 4—figure supplement 5. Inhibition of trypsins impairs the development of wasp larvae.

The length of the Td larvae in CK (H_2O) and TLCK-injected hosts after 96 h and 144 h parasitization. Left to right: n = 25, 24, 28 and 30 biologically independent larvae. Data represent the mean ± SEM. Significance was determined by two-way ANOVA with Sidak's multiple comparisons test (***$p < 0.001$).

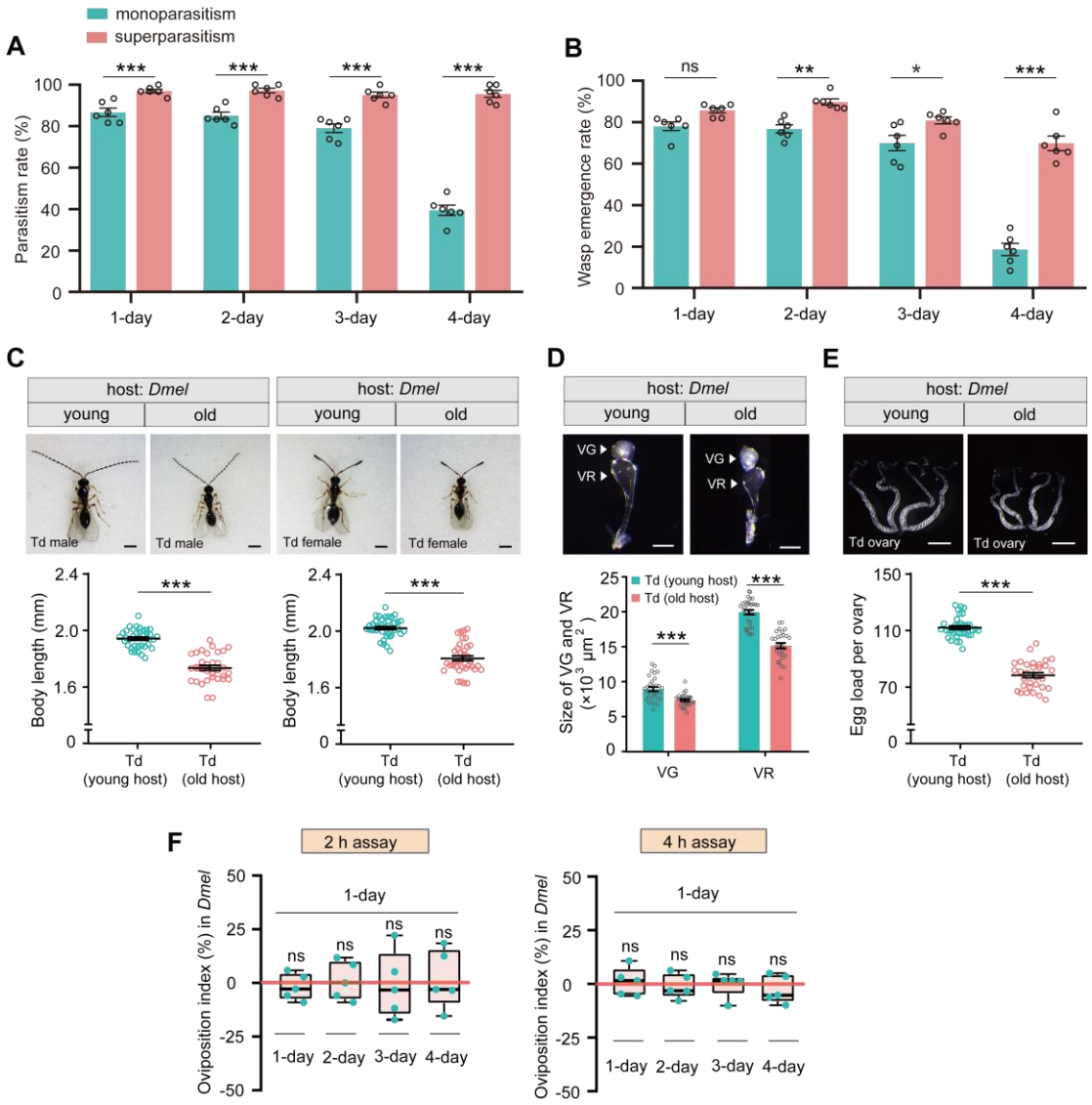

Figure 5—figure supplement 1. Superparasitism enhances Td parasitic efficiency on *D. melanogaster*.

(**A**) and (**B**) Parasitism rates (**A**) and wasp emergence rates (**B**) in 1- to 4-day-old *D. melanogaster* pupae after monoparasitism or superparasitism by Td. Six biological replicates were performed. Data represent the mean ±SEM. Significance was analyzed by two-way ANOVA with Sidak's multiple comparisons test (ns, not significant; *$p < 0.05$; **$p < 0.01$; ***$p < 0.001$). (**C**) The images and body length of Td males and females emerged from young and old *D. melanogaster* hosts. n = 40 and 36 male wasps, n = 35 and 33 female wasps, respectively. Data represent the mean ±SEM. Significance was determined by two-tailed unpaired Student's t tests (***$p < 0.001$). Scale bar: 500 μm. (**D**) The size of venom gland (VG) and venom reservoir (VR) of Td females emerged from young and old *D. melanogaster* hosts. Left to right: n = 32, 30, 32 and 30 wasps. Data represent the mean ±SEM. Significance was determined by two-tailed unpaired Student's t tests (***$p < 0.001$). Scale bar: 100 μm. (**E**) The ovaries and egg load of Td females emerged from young and old *D. melanogaster* hosts. n = 33 and 31 wasps, respectively. Data represent the mean ±SEM. Significance was determined by two-tailed unpaired Student's t tests (***$p < 0.001$). Scale

bar: 400 μm. (**F**) Oviposition indices of Td females in different aged *D. melanogaster* hosts from 2 h and 4 h assays. Five biological replicates were performed. Box plots represent the median (bold black line), quartiles (boxes), as well as the minimum and maximum (whiskers). All oviposition indices were not significantly different with zero (bold red line), which represents no choice for Td egg laying. Deviation of the oviposition index against zero was tested with Wilcoxon signed rank test (ns, not significant). Young host: 1-day-old pupae; old host: 4-day-old pupae.

Figure 5—figure supplement 2. The image of the host parasitized by two Td female wasps.

Two Td female wasps showed a collaboration to parasitize the same *D. suzukii* pupa. Scale bar: 500 μm.

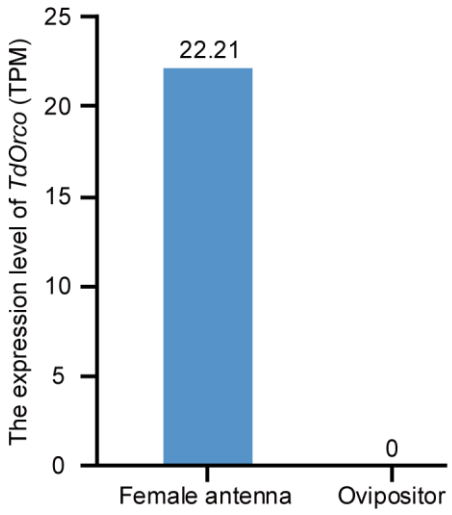

Figure 6—figure supplement 1. Transcriptome expression profile of *Orco* on female antenna and ovipositor of Td.